Supplementary Figures, Tables, Text and References

Supplementary Figure 1

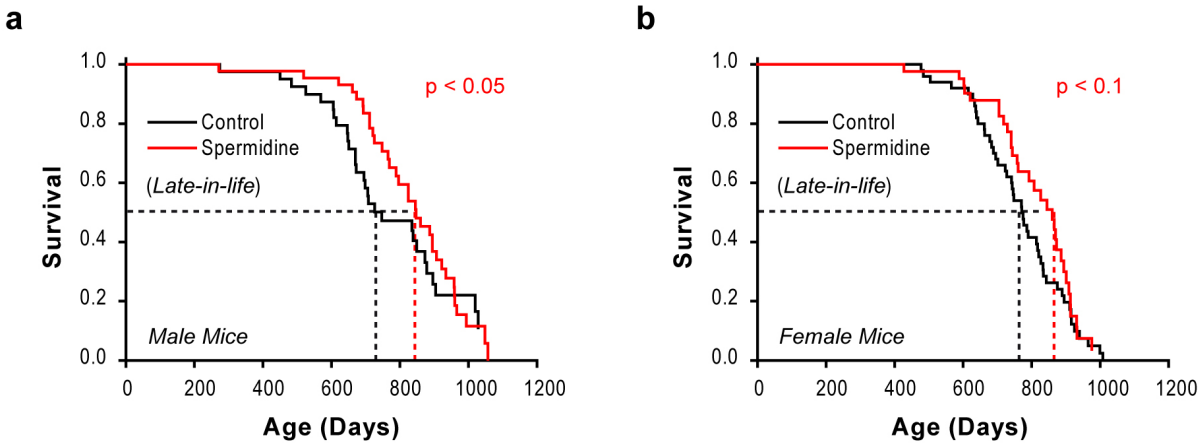

Supplementary Figure 1. Spermidine supplementation *late-in-life* shows comparable effects on longevity in male and female C57BL/6 mice.

Kaplan-Meier survival analysis of male **(a)** and female **(b)** aging C57BL/6J wild-type mice with *late-in-life* supplementation of spermidine (see Fig. 1a, d). Mice received standard chow and autoclaved water *ad libitum*. Dashed lines depict median lifespans. N=41/44 (**a**, control/spermidine) male mice and N=50/42 (**b**, control/spermidine) female mice. P-value represents comparison with control group calculated using Breslow test.

Supplementary Figure 2

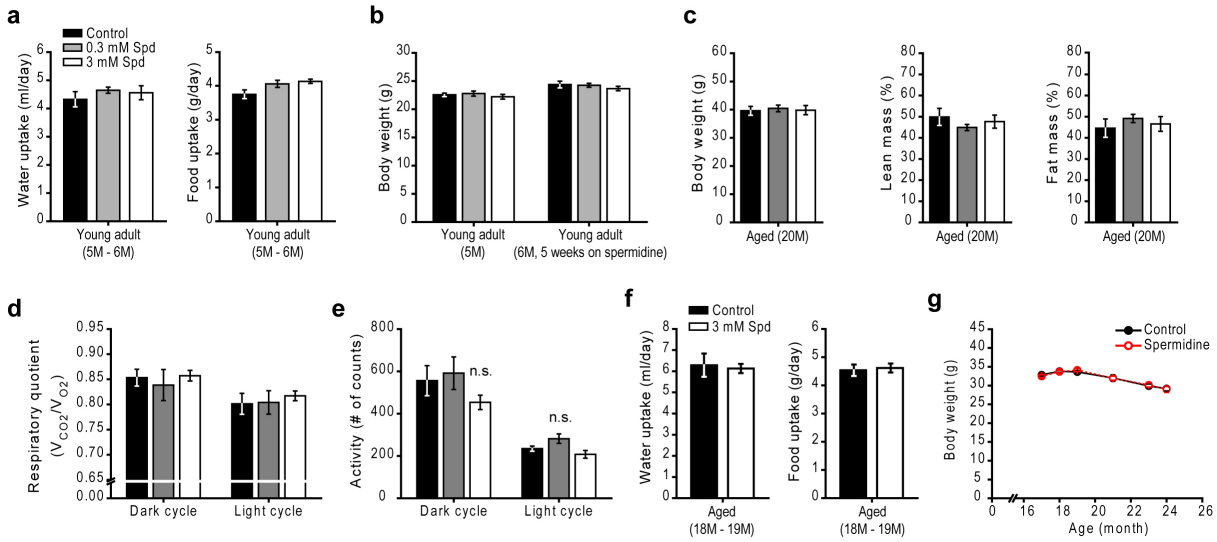

Supplementary Figure 2. Food and water uptakes, body weight and body composition are not affected by spermidine supplementation in young and aged mice.

Spermidine (Spd) was supplemented to drinking water either early-in-life, *life-long* or *late-in-life* (see Fig. 1a for the feeding scheme) **(a, b)** Food and water consumptions (a) as well as body weight (b), determined before (left) and after (right) the period of food and water consumption recordings of young wild-type C57BL/6N female mice with and without Spd supplementation in drinking water. Food and water consumptions were recorded and averaged over a period of 5 weeks (at indicated ages in months, M). N=4 cages/group with each cage containing 5 mice. **(c-e)** Body weight as well as body fat and lean mass percentages (c), respiratory quotient (d) and general activity (e) of aged (20M) wild-type C57BL/6N female mice after *life-long* supplementation of spermidine. N=12 (c) and N=11-12 (d, e) mice/group. **(f, g)** Food and water consumptions (f) as well as body weight (g) of *late-in-life* spermidine-supplemented aged wild-type C57BL/6J male mice compared with age-matched controls at the indicated ages. N=9 cages/group with each cage containing 4 mice (f), N=14-36 mice/group and time point (g). Data are presented as means ± s.e.m..

Supplementary Figure 3

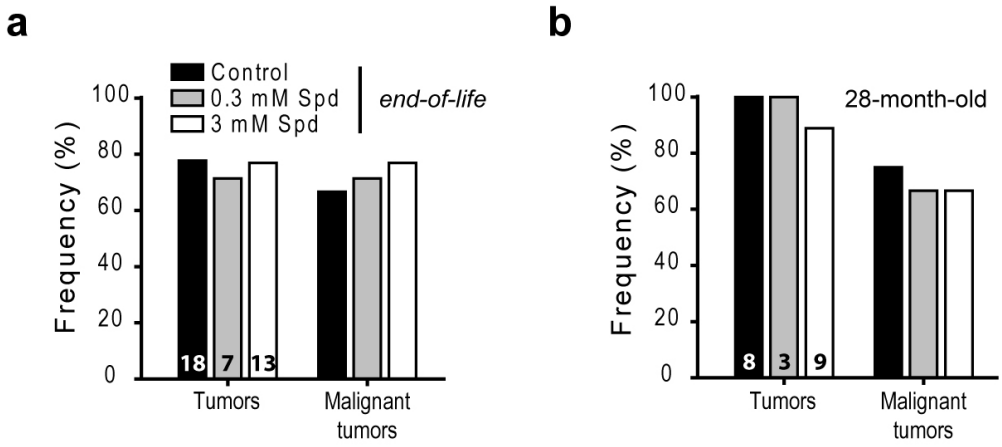

Supplementary Figure 3. Tumor incidence is not affected by spermidine treatment in aged mice.

Tumor incidence determined by pathological analyses of **(a)** "*end-of-life*" animals (sacrificed close before their natural death; see Methods section for the *end-of-life determination* criteria) and **(b)** 28-month-old mice after *life-long* supplementation of spermidine (Spd) to drinking water at indicated concentrations and compared to respective untreated controls (see Fig. 1a for the feeding scheme). Data show the relative fraction of tumor incidences (in %), which were not significantly different between the groups as tested by binomial logistic regression. Numbers in bars indicate the number of mice analyzed. Malignant tumors were defined according to "WHO International Classification of Rodent Tumors", Ref.: *International Classification of Rodent Tumors. The Mouse*. (Mohr, Ulrich (Ed.), Springer Berlin Heidelberg, 2001).

Supplementary Figure 4

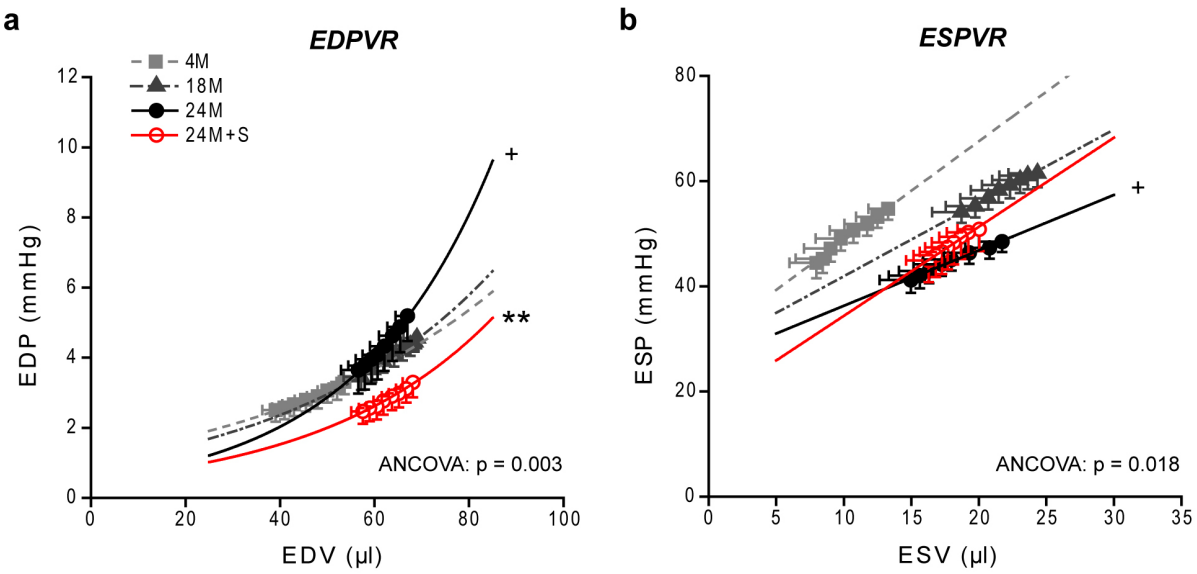

Supplementary Figure 4. Spermidine improves cardiac diastolic function by reducing left ventricular passive stiffness in aging C57BL/6J mice.

Cardiac function was assessed by left ventricular pressure-volume measurements in young (4M), middle-aged (18M), aged (24M) and aged with *late-in-life* spermidine supplementation (24M+S) C57BL/6J wild-type mice (see Fig. 1a for the feeding scheme). Graphs show exponential end-diastolic and linear end-systolic pressure-volume relationships, EDPVR **(a)** and ESPVR **(b)**, respectively, obtained by inferior *vena cava* occlusion that was performed on 8-10 mice/group. *Note the upward shift of EDPVR (increased passive stiffness) in 24M compared with 4M and the downward shift (reduced passive stiffness) in 24M+S compared with 24M.* $^{+}p<0.05$ *vs.* 4M, $^{**}p<0.01$ *vs.* 24M control (ANCOVA with Bonferroni post-hoc). For more details, please refer to Fig. 1g-i, k, Supplementary Table 6 and Methods section.

Supplementary Figure 5

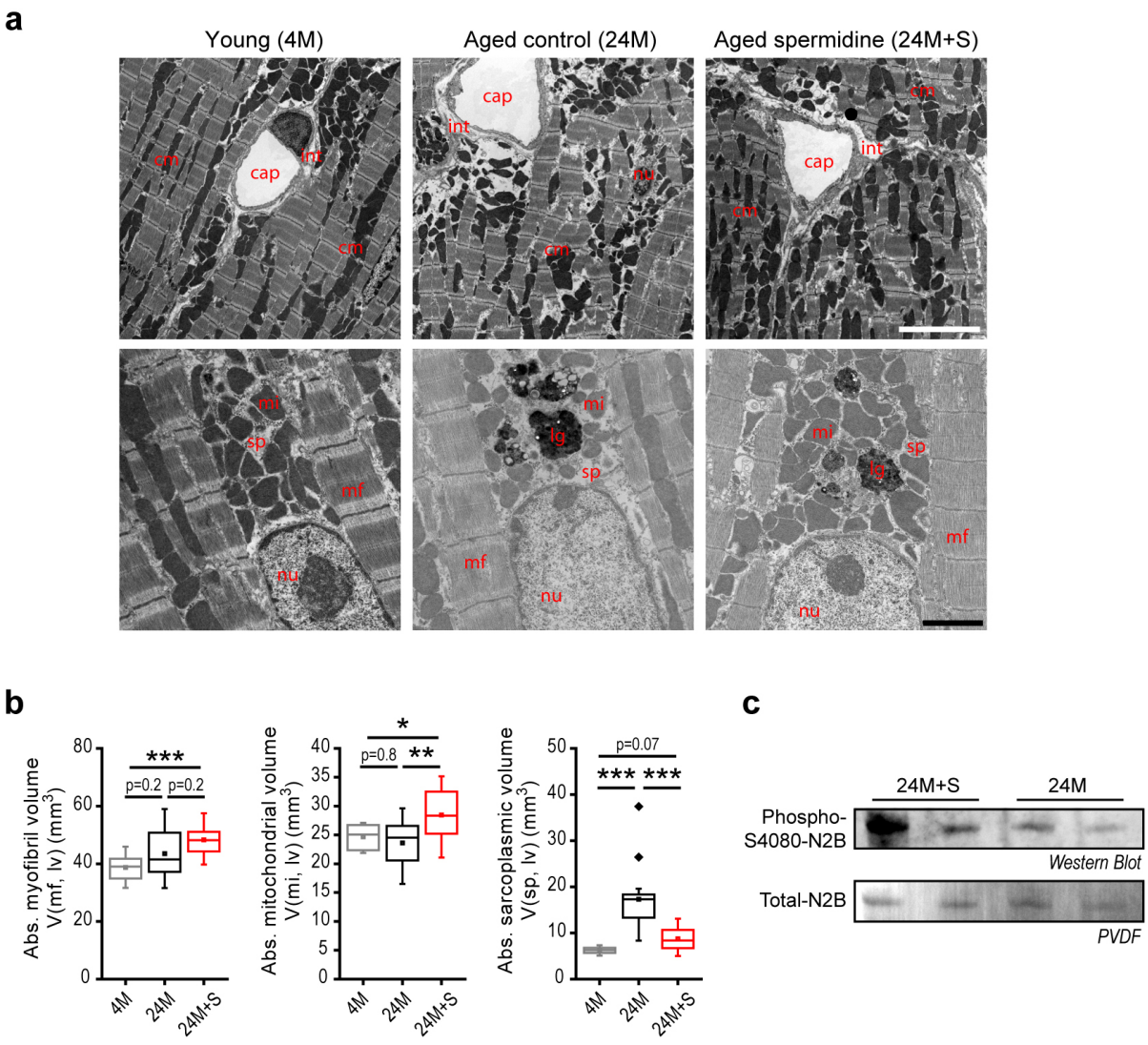

Supplementary Figure 5. Ultrastructure of cardiomyocytes reveals increased mitochondrial and myofibrillar volume induced by spermidine in aged mice.

(a) Representative transmission electron micrographs of left ventricular samples from young (4M), aged (24M) and aged *late-in-life* spermidine-treated (24M+S) C57BL/6J male mice (see Fig. 1a for the feeding scheme). Abbreviations: cap, capillary; cm, cardiomyocyte; int, interstitium; lg, lipofuscin granules; mf, myofibrils; mi, mitochondria; nu, nucleus; sp, sarcoplasm. Scale bars represent 5 µm (upper panels) and 2 µm (lower panels). **(b)** Quantification of absolute left ventricular myofibril volume, *V(mf, lv)*, mitochondrial volume, *V(mi, lv)* as well as mitochondria- and myofibril-free sarcoplasmic volume, *V(sp, lv)*, using design-based stereology. Data are presented as box-plots with whiskers showing minima and maxima within 1.5 interquartile range. N=10/15/14 (4M/24M/24M+S) mice. ***p<0.001, **p<0.01 using ANOVA with post-hoc Tukey, V(mf, lv), Welch's test with post-hoc Games-Howell, V(mi, lv) or Kruskal-Wallis with corrected multiple-comparisons by Mann-Whitney U-test, V(sp, lv), according to normality and equality of variances (for details, please refer to Methods section) **(c)** Representative *Western Blot* probed with phospho-serine 4080-specific N2B antibody (Phospho-S4080-N2B) and *PVDF* membrane showing total amounts of N2B (*Total-N2B*). See Fig. 2 for quantifications.

Supplementary Figure 6

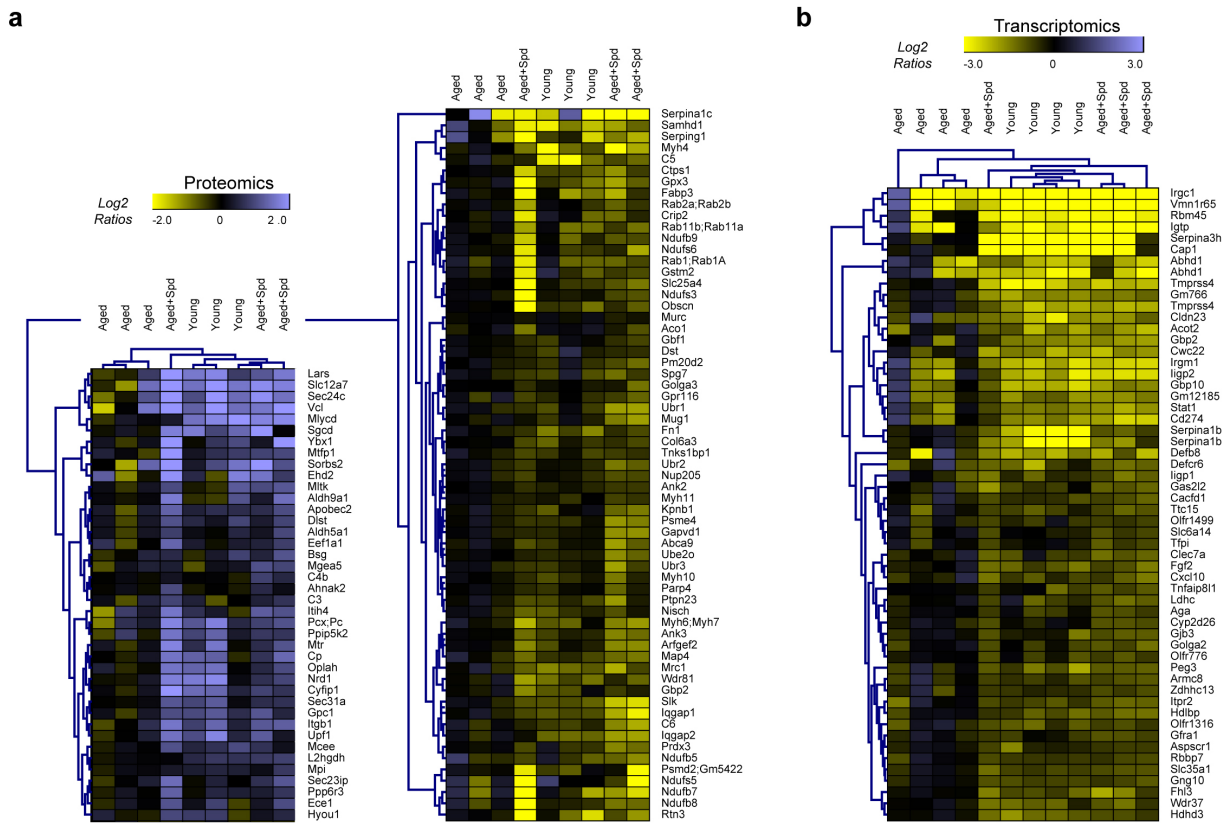

Supplementary Figure 6. Spermidine rejuvenates the molecular profile of aged mouse hearts.

(a) Proteome analysis of cardiac tissue extracts from overnight-fasted 23-month-old C57BL/6J male mice receiving *late-in-life* spermidine supplementation (Aged+Spd) compared to age-matched (Aged) as well as young (Young) controls using label-free mass spectrometry. N=3 mice/group. Ten percent most reproducible changes in protein ratios (Aged+Spd *vs.* Aged) are depicted (*log2 ratios*) and compared to Young ratios. **(b)** Cardiac transcriptome analysis from 30-32-month-old *life-long* spermidine-treated C57BL/6N female mice compared to untreated and young controls. Significant changes in protein ratios (Aged+Spd *vs.* Aged) are depicted (*log2 ratios*) and compared to Young ratios. N=4 mice/group. *Hierarchical clustering revealed that spermidine-treated mice resembled proteomic and transcriptomic profiles of young animals.*

Supplementary Figure 7

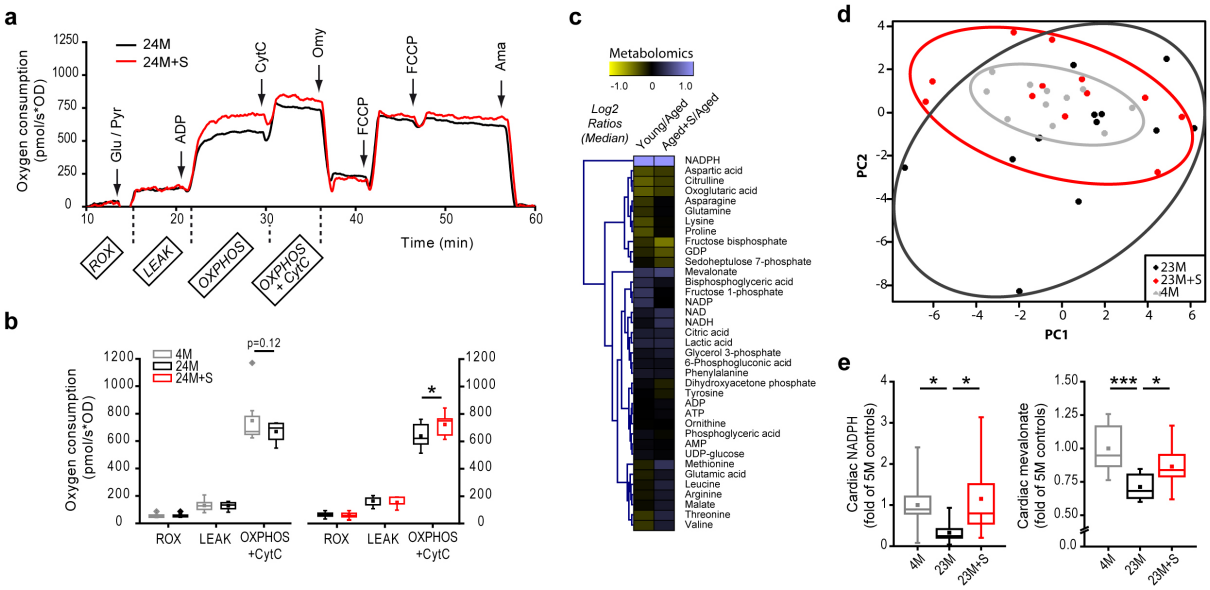

Supplementary Figure 7. Improved metabolomic profile and mitochondrial respiratory function by spermidine in aged mouse hearts.

(a, b) Representative oxygraph recordings (a) and quantification (b) of mitochondrial respiration from isolated cardiac mitochondria incubated with complex I supplying substrates glycine and pyruvate (Gly/Pyr). *ROX*, Residual respiration (*State 1)* in the absence of reduced substrate and ADP; *LEAK,* Respiration compensating for proton leak in the absence of ADP but presence of reduced substrate; *OXPHOS*, ADP-stimulated respiration of coupled mitochondria (quantification shown in Fig. 2c); *OXPHOS+CytC,* Oxphos after addition of cytochrome C. Oligomycin (Omy), FCCP, antimycin A (ama) were added as controls to block respiration by inhibition of ATP synthase, induce maximum respiration through uncoupling and block uncoupled respiration by complex III inhibition, respectively. N=8/8 (4M/24M) and N=5/5 (24M/24M+S) mice. *p<0.05 (Paired Student's *t*-test). **(c, d)** Metabolome analyses of cardiac tissue extracts from overnight-fasted wild-type animals with *late-in-life* spermidine supplementation (23M+S) compared to age-matched (23M) as well as young (4M) controls (see Fig. 1a for the feeding scheme). Median ratios (c) of metabolite alterations and principal component analysis (d) obtained from 12 animals are shown. Manually added ellipsoid lines in (d) circumscribe the distribution of the groups. Variance explained by PC1 and PC2: 40%. **(e)** Relative cardiac NADPH and mevalonate levels obtained from metabolomics data presented in (c, d). Values were normalized to young controls (see Methods for details). N=12/11/11 (left) and N=12/12/12 (right) (4M/23M/23M+S) mice. ***p<0.01, *p<0.05 (ANOVA, post-hoc Tukey). For box-and-whisker plots, whiskers show minima and maxima within 1.5 interquartile range.

Supplementary Figure 8

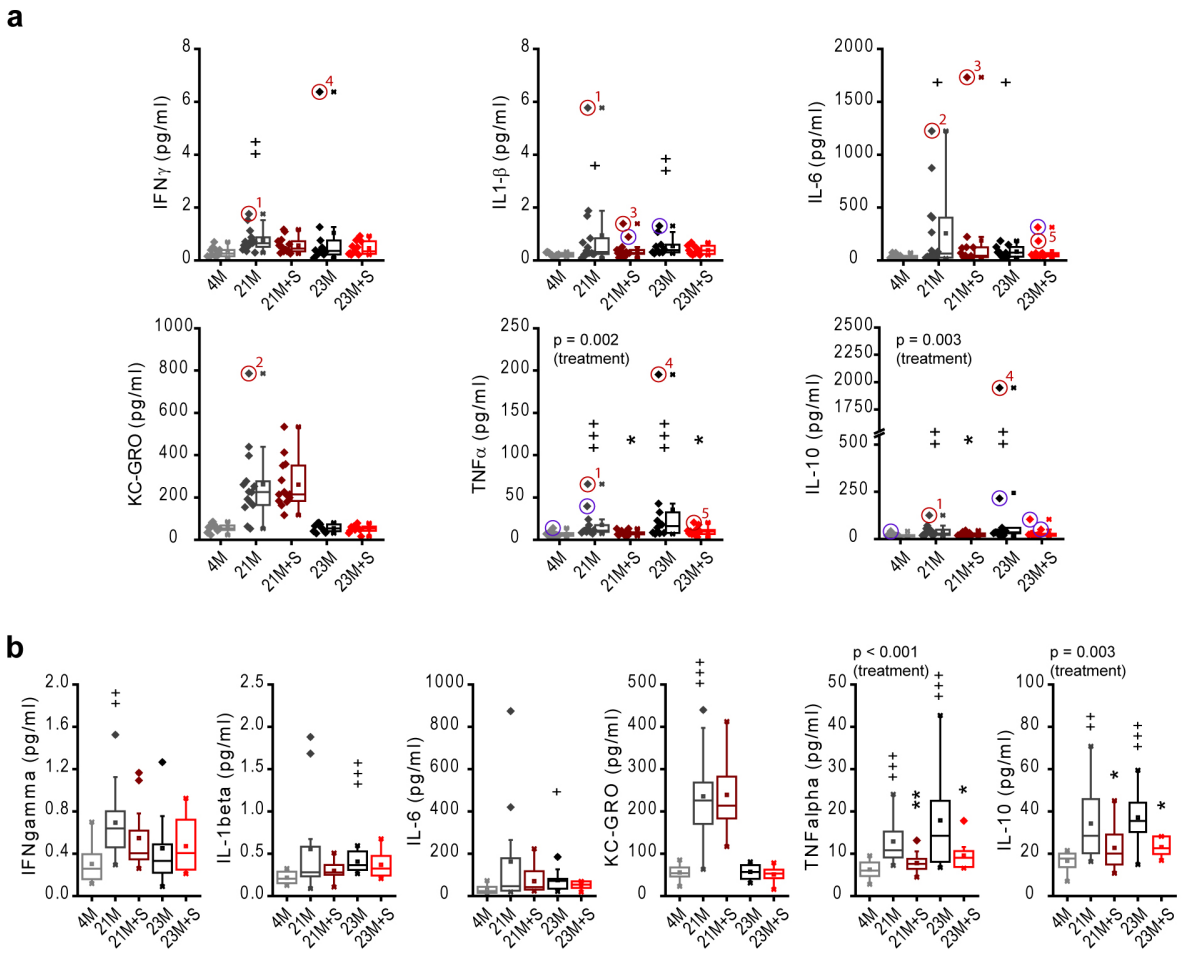

Supplementary Figure 8. Spermidine suppresses age-induced subclinical systemic inflammation in mice.

Plasma cytokine levels assessed by electrochemiluminescence-based immunoassays from late-in-life spermidine-treated (+S) animals (see Fig. 1a for the feeding scheme). **(a)** Subclinical inflammatory cytokine levels (including all data points) along with the outlier analysis applied to define (chronic) low-grade inflammatory status, which is shown in (b). N=12/14/14/10/11 (4M/21M/21M+S/23M/23M+S) mice. Data are presented as box-plots with whiskers showing minima and maxima within 2.2 interquartile range along with the outliers beyond that range. Red circles depict outliers in animals (numbered 1-5) with potential acute inflammatory condition, while purple circles show outliers in animals with a single cytokine outlier value (see Methods). **(b)** Low-grade (chronic) inflammatory cytokine levels obtained by (i) excluding animals with potential acute inflammatory condition as defined by having two or more statistically-identified (2.2-fold IQR labelling rule) outlier values (red circles in a) and (ii) winsorizing outliers in animals with a single cytokine outlier value (purple circles in a). N=12/12/13/9/10 (4M/21M/21M+S/23M/23M+S) mice. Data are presented as box-plots with whiskers showing minima and maxima within 1.5 interquartile range.

P-values indicate factor comparisons by two-way ANOVA including all 21M and 23M groups. **p<0.01, *p<0.05 vs. age-matched control (simple main effects).

+++p<0.001, ++p<0.01, +p<0.05 vs. 4 month-old control (ANOVA with post-hoc Tukey, Welch's test with post-hoc Games-Howell or Kruskal-Wallis followed by corrected multiple comparisons by Mann-Whitney U-test according to normality and equality of variances).

Supplementary Figure 9

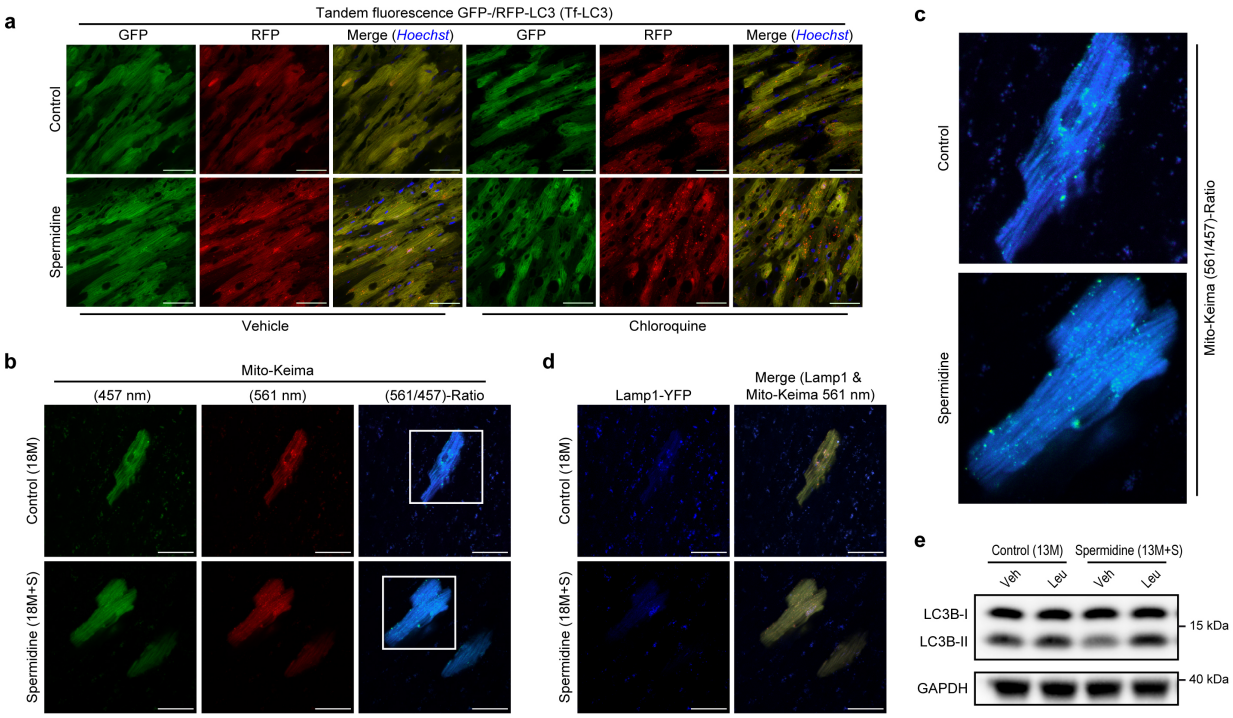

Supplementary Figure 9. Cardiac autophagy and mitophagy is induced by spermidine in mice.

(a) Young (3-month-old) transgenic male mice harboring cardiac-specific expressed tandem-fluorescence mRFP-GFP-LC3 (tf-LC3) were subjected to spermidine treatment for 2 weeks and hearts were analyzed by confocal microscopy 4 hours after injection of chloroquine or vehicle to assess autophagic flux. Representative confocal images are shown. Orange puncta in merged images represent autophagosomes, while red puncta indicate autolysosomes. Nuclei were visualized by *Hoechst* staining. Scale bars represent 50 µm. **(b-d)** Evaluation of mitophagy by AAV9-Mito-Keima and AAV9-Lamp1-YFP injected to aged (18-month-old) C57BL/6J wild-type male mice. Hearts were examined after 3 weeks of spermidine supplementation and compared to age-matched controls. Panel b shows representative images of Mito-Keima excited at 457 nm (shown in green color) or at 561 nm (shown in red color) as well as a ratiometric image (561 nm/457 nm excitation, shown in blue color). Panel c shows enlargement of marked areas in (b). *Notice the higher ratiometric signal (defined as Mito-Keima positive area), indicating higher mitophagy in spermidine-treated versus control animals*. Panel d depicts Lamp1-YFP (blue color) and the merged image of Mito-Keima fluorescence excited at 561 nm (red color) and Lamp1-YFP (blue color). Scale bars represent 50 µm. **(e)** Assessment of autophagic flux by LC3 immunoblotting after intra-peritoneal injection of leupeptin (Leu) or vehicle (Veh) in 13-month-old C57BL/6J wild-type mice supplemented for 4 weeks with spermidine. Representative immunoblot probed with LC3- or GAPDH-specific antibodies is shown.

Supplementary Figure 10

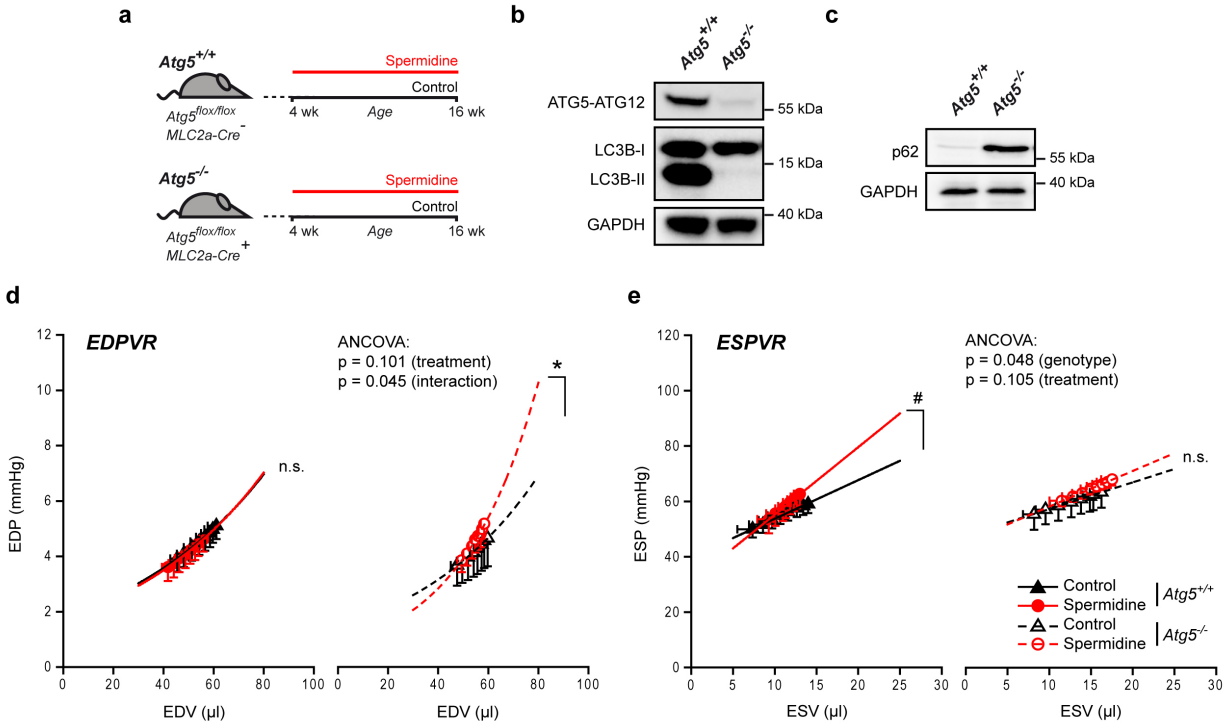

Supplementary Figure 10. Spermidine aggravates cardiac diastolic function in cardiomyocyte-specific Atg5-deficient mice.

Cardiac function was assessed by left ventricular pressure-volume measurements in control and spermidine-treated *Atg5$^{flox/flox}$/MLC2a-Cre^{-}* (*Atg5$^{+/+}$*) and *Atg5$^{flox/flox}$/MLC2a-Cre^{+}* (*Atg5$^{-/-}$*) mice at the age of 16 weeks. **(a)** Scheme depicting experimental design. Spermidine (3 mM) was supplemented to drinking water from the age of 4 weeks (after weaning) until the assessment of cardiac function **(b, c)** Representative immunoblot analysis confirming deletion of *Atg5* and autophagy incompetence in isolated ventricular cardiomyocytes of *Atg5$^{-/-}$* mice. Protein extracts from isolated cardiomyocytes obtained from 16-week-old animals were subjected to SDS-page and probed with antibodies against Atg5, LC3 and GAPDH, as a loading control, (b) or p62 and GAPDH, as a loading control, (c). **(d-e)** Exponential end-diastolic and linear end-systolic pressure-volume relationships, EDPVR (d) and ESPVR (e), respectively, obtained by inferior *vena cava* occlusion performed on 9-11 mice/group. *Note the steeper slope of ESPVR (improved contractility) in spermidine-treated Atg5$^{+/+}$ mice compared with genotype-matched controls and the ESPVR rightward shift (impaired contractility) in both Atg5$^{-/-}$ groups, especially the spermidine-treated, compared with Atg5$^{+/+}$ groups. Also note the upward shift of EDPVR (increased passive stiffness) in spermidine-fed Atg5$^{-/-}$ mice compared with genotype-matched controls.* Indicated p-values represent factor comparisons by two-way ANCOVA. $^{\#}$p<0.06, *p<0.05 *vs.* respective control (simple main effects). For more details, please refer to Fig. 3g-h, Supplementary Table 12 and Methods section.

Supplementary Figure 11

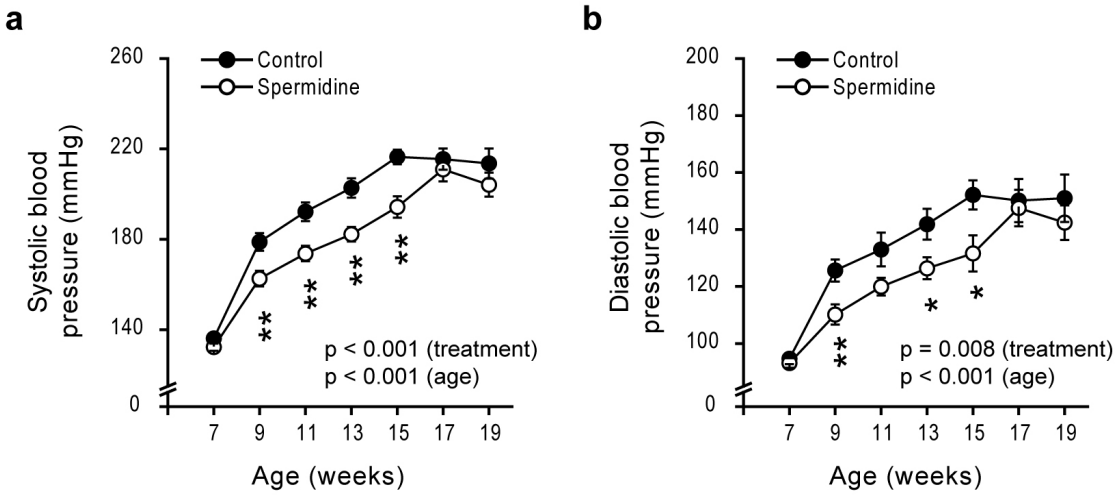

Supplementary Figure 11. Spermidine delays high-salt diet-induced increase in systolic and diastolic blood pressures.

Systolic **(a)** and diastolic **(b)** blood pressures assessed by non-invasive tail-cuff method in spermidine-fed vs. control *Dahl* salt-sensitive rats receiving high-salt diet (see Fig. 4a for the feeding scheme). Data show means ± s.e.m. (N=10 rats/group). P-values represent factor comparisons calculated by mixed two-way ANOVA. **p<0.01, *p<0.05 *vs.* age-matched control (simple main effects).

Supplementary Figure 12

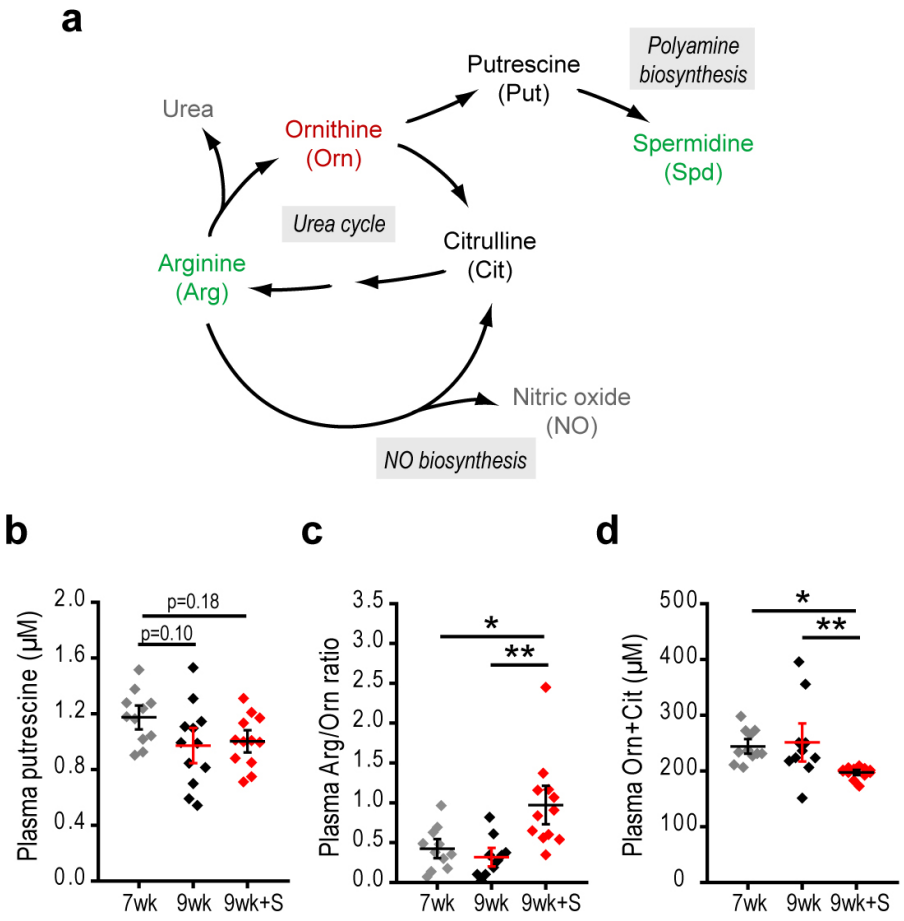

Supplementary Figure 12. Spermidine increases arginine and NO bioavailability via altering ornithine metabolism in *Dahl* salt-sensitive rats.

(a) Simplified scheme depicting the interconnection of arginine metabolism (urea cycle) with polyamine and nitric oxide (NO) biosynthesis pathways. **(b)** Plasma levels of putrescine, **(c)** plasma arginine/ ornithine ratio (Arg/Orn ratio) and **(d)** plasma levels of ornithine and citrulline combined (Orn+Cit) of spermidine-fed (+S) *Dahl* salt-sensitive rats compared with controls calculated from HPLC/MS- (ornithine) and HPLC-based (arginine and citrulline) quantification of plasma metabolite concentrations. N=11/12/12 (b) and N=11/10/12 (c, d) (7wk/9wk/9wk+S) rats. Data are presented as box-plots with whiskers showing minima and maxima within 1.5 interquartile range. **p<0.01, *p<0.05 (ANOVA, post-hoc Tukey). Wk, weeks.

Supplementary Figure 13

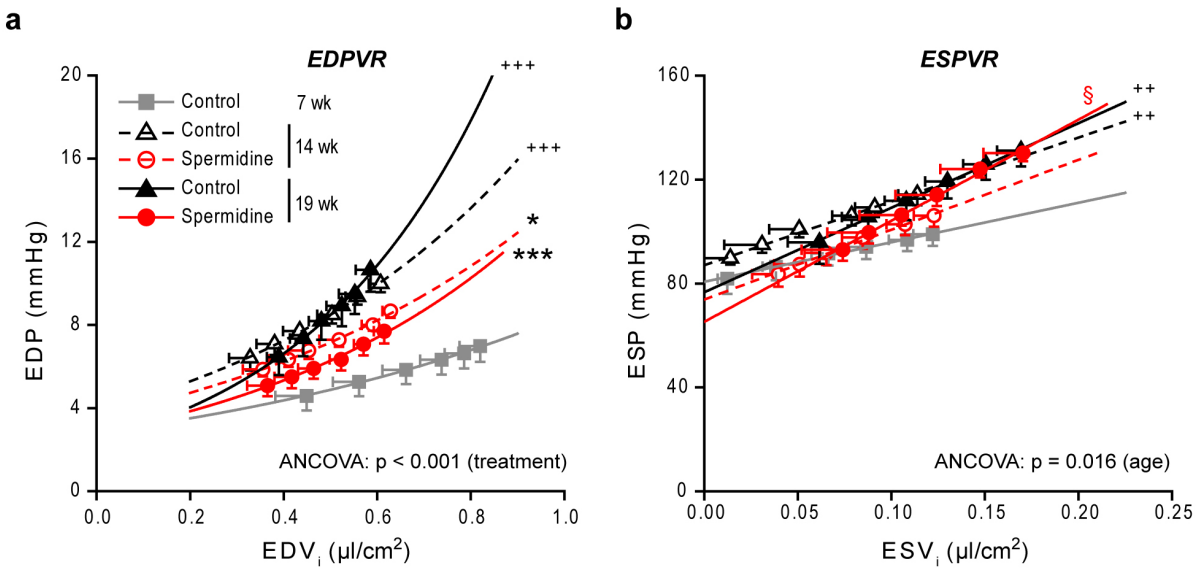

Supplementary Figure 13. Spermidine improves cardiac diastolic function by reducing left ventricular stiffness in high-salt diet-fed *Dahl* salt-sensitive rats.

Cardiac function was assessed by left ventricular pressure-volume measurements in *Dahl* salt-sensitive rats fed a high-salt diet starting from the age of 7 weeks (see Fig. 4a for the feeding scheme) with a subset of rats co-administrated with spermidine in drinking water. Exponential end-diastolic and linear end-systolic pressure-volume relationships, EDPVR **(a)** and ESPVR **(b)**, respectively, obtained by inferior *vena cava* occlusion performed on 9-10 rats/group are depicted with volumes indexed to body surface area to account for differences in body size (see Methods section). *Note the upward shift of EDPVR (increased passive stiffness) in 14 and 19 wk controls compared with 7 wk control and the downward shift (decreased passive stiffness) in spermidine-treated 14 and 19 wk animals compared with their age-matched controls.*

P-values represent factor comparisons by two-way ANCOVA including all 14 and 19 wk groups. ***p<0.001, *p<0.05 *vs.* age-matched control (simple main effects).

§p<0.05 *vs.* treatment-matched 14 wk (simple main effects); $^{+++}$p<0.001, $^{++}$p<0.01 *vs.* 7 wk control (ANCOVA comparing controls with post-hoc Bonferroni). For more details, please refer to Fig. 4f-h, k, Supplementary Table 15 and Methods section.

Supplementary Figure 14

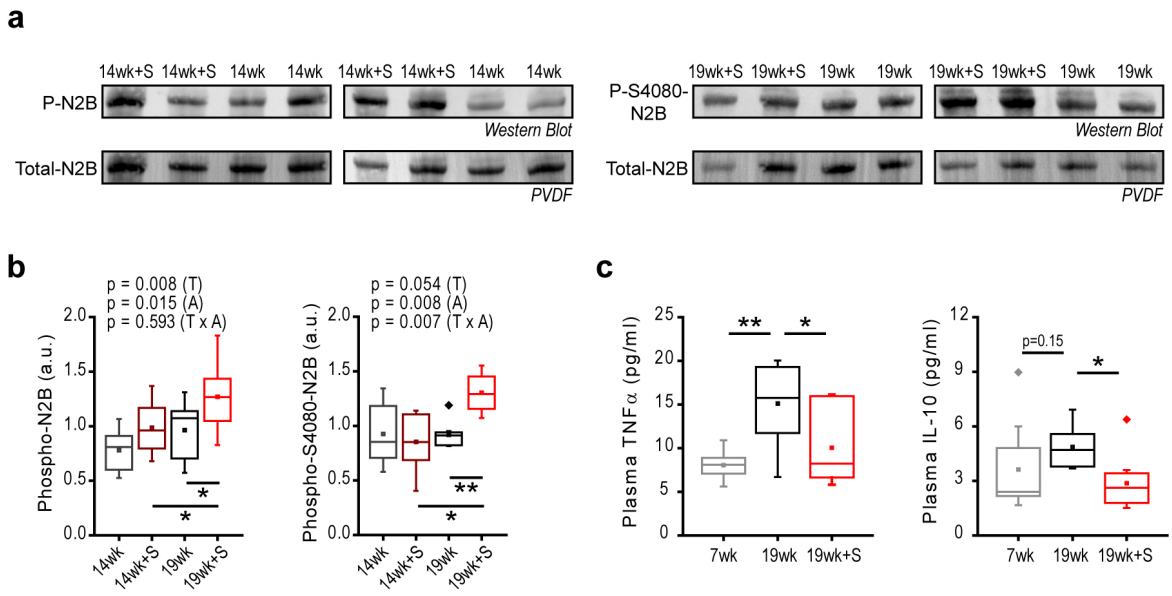

Supplementary Figure 14. Spermidine increases titin-phosphorylation and suppresses circulating levels of TNFα in Dahl salt-sensitive rats.

Dahl salt-sensitive rats were fed a high-salt diet starting from the age of 7 weeks with a subset of rats co-administered with spermidine (+S) in the drinking water (see Fig. 4a for the feeding scheme). Cardiac tissue extracts (a, b) or plasma obtained from EDTA-collected blood (c) were analyzed at the indicated ages. **(a, b)** Representative *Western Blots* (a) probed with pan-phospho-serine/threonine- or Phospho-S4080-N2B-specific antibodies depicting N2B phosphorylation (P-N2B and P-S4080-N2B, respectively). *PVDF* membrane shows total amounts of N2B (*Total-N2B*). Blots/membranes were quantified by densitometry (b) using normalization standards for inter-gel comparisons (see Methods). N=8 rats/group. P-values represent factor (T, treatment; A, age) comparisons by two-way ANOVA. **p<0.01, *p<0.05 (simple main effects). **(c)** Plasma cytokine levels assessed by electrochemiluminescence-based immunoassays. N=12/7/10 (7wk/19wk/19wk+S) rats. **p<0.01, *p<0.05 (ANOVA, post-hoc Tukey). For box-and-whisker plots, whiskers show minima and maxima within 1.5 interquartile range. Wk, weeks.

Supplementary Figure 15

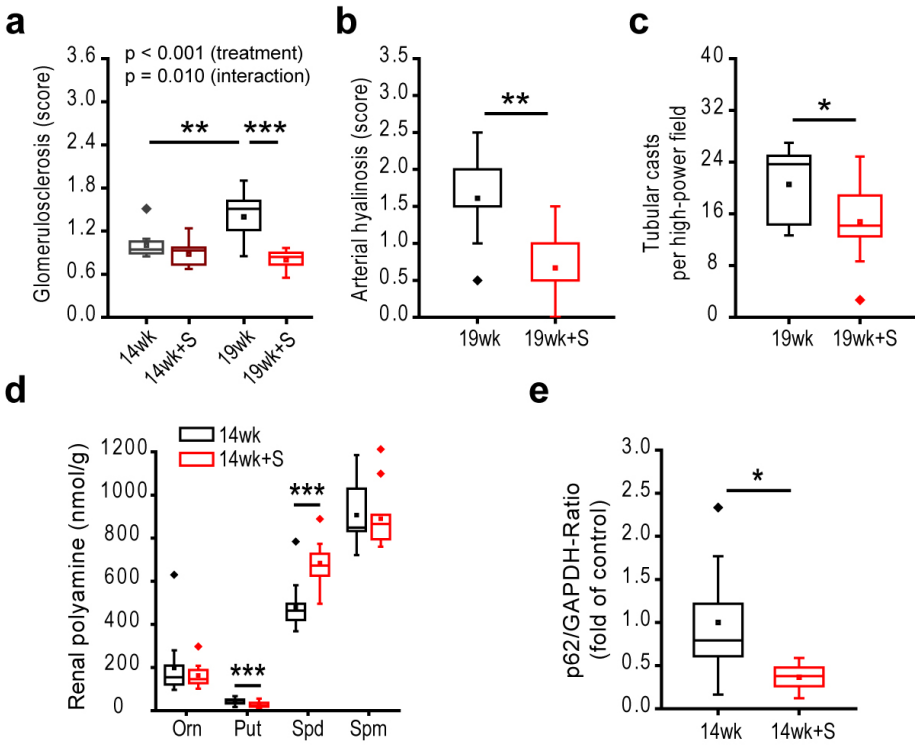

Supplementary Figure 15. Spermidine protects from salt-induced kidney damage in *Dahl* salt-sensitive rats.

(a-c) Glomerulosclerosis (a) and arterial hyalinosis (b) were analyzed at indicated ages semi-quantitatively (*score*-based evaluation) on PAS-stained renal tissue obtained from high-salt diet-fed *Dahl* salt-sensitive rats with a subset of rats co-administered with spermidine (+S) in the drinking water (see Fig. 4a for the feeding scheme). The number of renal tubular casts (c) was counted in 6 high-power fields. N=9 rats/group. **(d)** Kidney polyamines content in 14-week-old rats. Orn, ornithine; Put, putrescine; Spd, spermidine; Spm, spermine. N=13/11 (14wk/14wk+S) **(e)** Densitometric quantification of immunoblot signals obtained from kidney protein extracts (14-week-old rats) probed with p62- and GAPDH-specific antibodies. p62 signals were normalized to GAPDH, which served as a loading control. N=9/12 (14wk/14wk+S). Indicated p-values represent factor comparisons by two-way ANOVA (panel a). ***p<0.001, **p<0.01, *p<0.05 (Student's *t*-test). Data are presented as box-plots with whiskers showing minima and maxima within 1.5 interquartile range. Wk, weeks.

Supplementary Figure 16

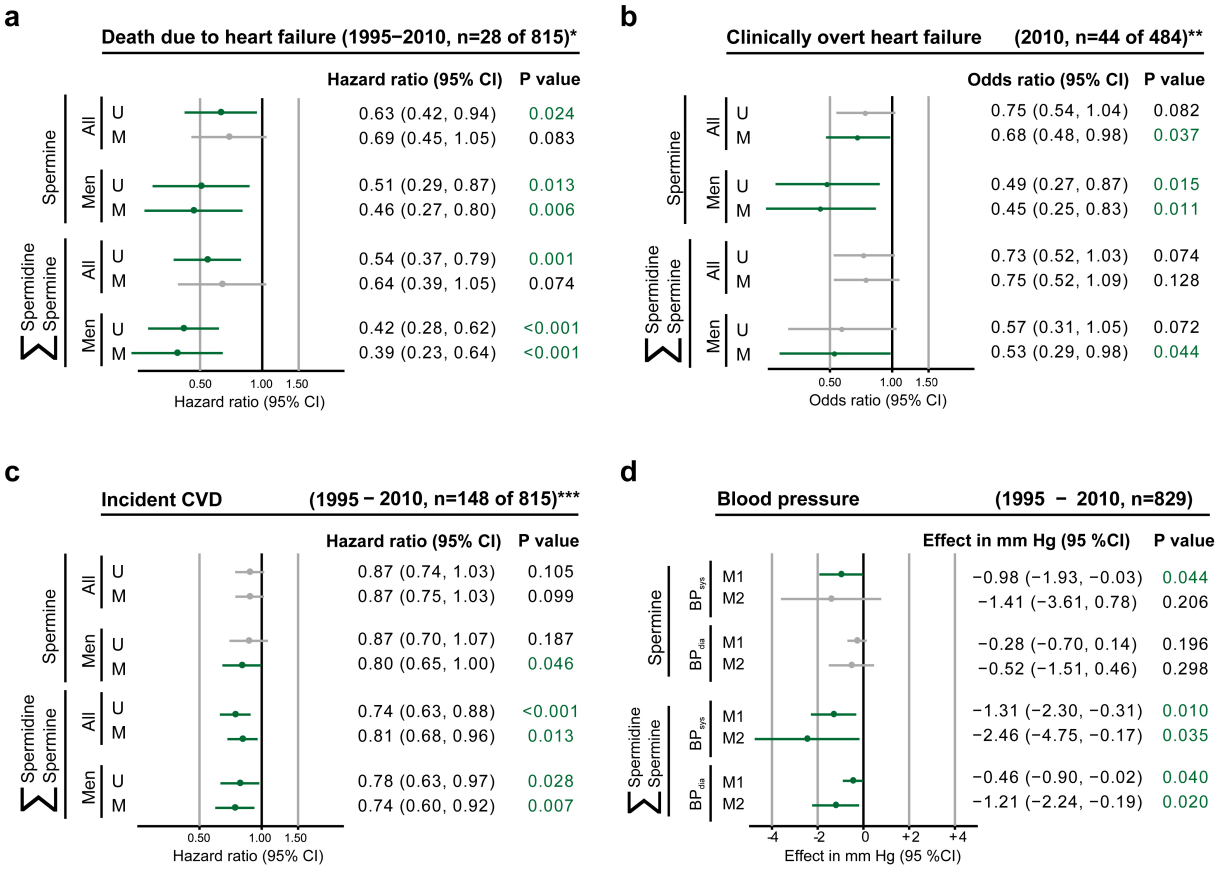

Supplementary Figure 16. Dietary polyamines inversely correlate with human cardiovascular disease.

(a-c) Associations of polyamine intakes (spermine or sum of spermine and spermidine) with (a) death due to heart failure, (b) clinically overt heart failure and (c) incident cardiovascular disease (CVD, composite of acute coronary artery disease, stroke and death due to vascular disease) in humans. Hazard ratios (panels a and c, time-to-event analysis) and odds ratios (panel b, cross-sectional analysis) are for one standard deviation higher intakes in given polyamines. Models were unadjusted (U) or had multivariable adjustment (M) for age, sex, total caloric intake, current smoking, diabetes, alcohol consumption, and diastolic blood pressure. *Death due to heart failure was defined according to ICD codes I50.x, I13.0, I13.2, I11.00, I11.01, or I97.1 and the results represent sub-distribution hazard ratios based on the Fine and Gray model and account for the competing risk of death due to causes unrelated to heart failure. **Diagnosis of heart failure (ascertained in 2010) relied on gold standard Framingham criteria. ***See methods for incident CVD criteria. **(d)** Associations of polyamine intakes (spermine or sum of spermine and spermidine) with systolic (BPsys) and diastolic (BPdia) blood pressures repeatedly assessed between 1995 and 2010 in 829 participants of the Bruneck Study. Effects represent the average difference in blood pressure (mmHg) associated with a one standard deviation higher intake of given polyamines (M1) or between the first and third tertile group (M2) under adjustment for age, sex, and total caloric intake.

Supplementary Figure 17

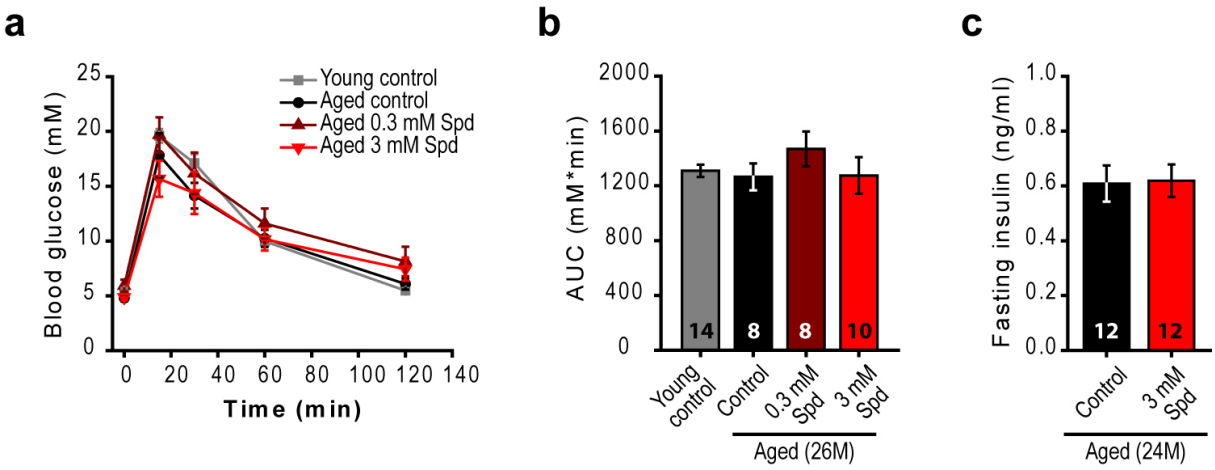

Supplementary Figure 17. Glucose and insulin metabolism are not affected by dietary spermidine supplementation in aging C57BL/6 mice.

(a) Blood glucose levels and **(b)** *area under the curve* (AUC) of intra-peritoneal glucose tolerance test (i.p. GTT) in C57BL/6N female mice with *life-long* supplementation of spermidine (Spd) in the drinking water (see Fig. 1a for the feeding scheme) compared to young (5M) or age-matched (26M) controls (M, month). **(c)** Plasma insulin levels after 3 hours of fasting in 24-month-old C57BL/6J male mice supplemented with Spd for 10 months or in age-matched controls. Data show means±s.e.m. with number of mice indicated in the bars.

Supplementary Figure 18

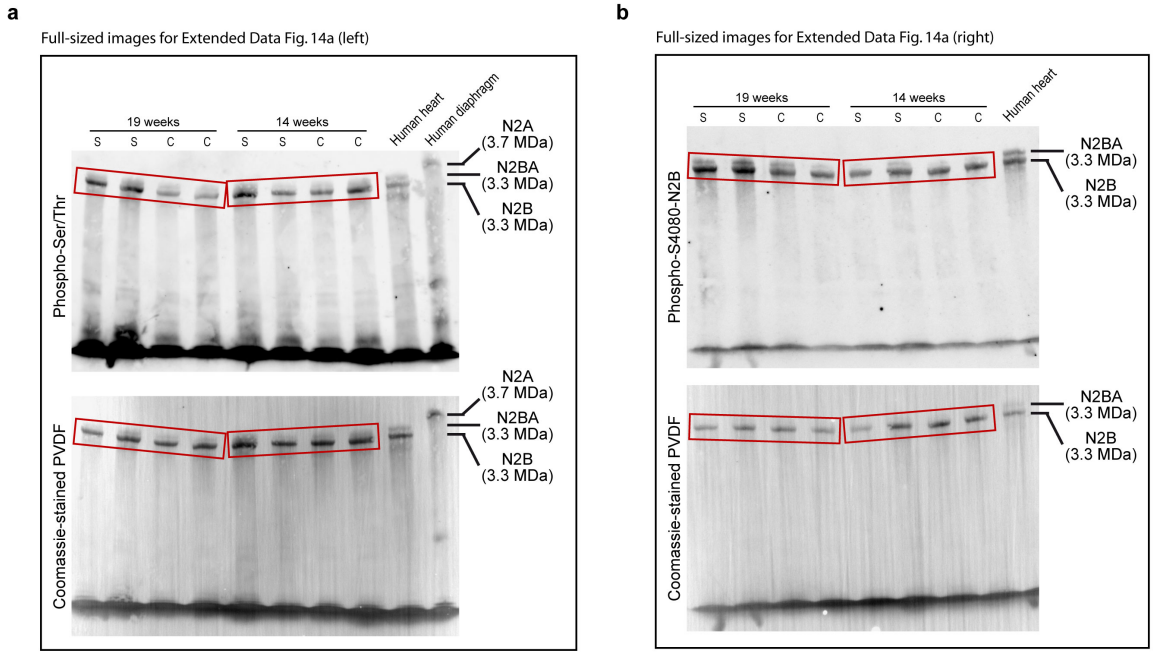

… Figure continued on the following page.

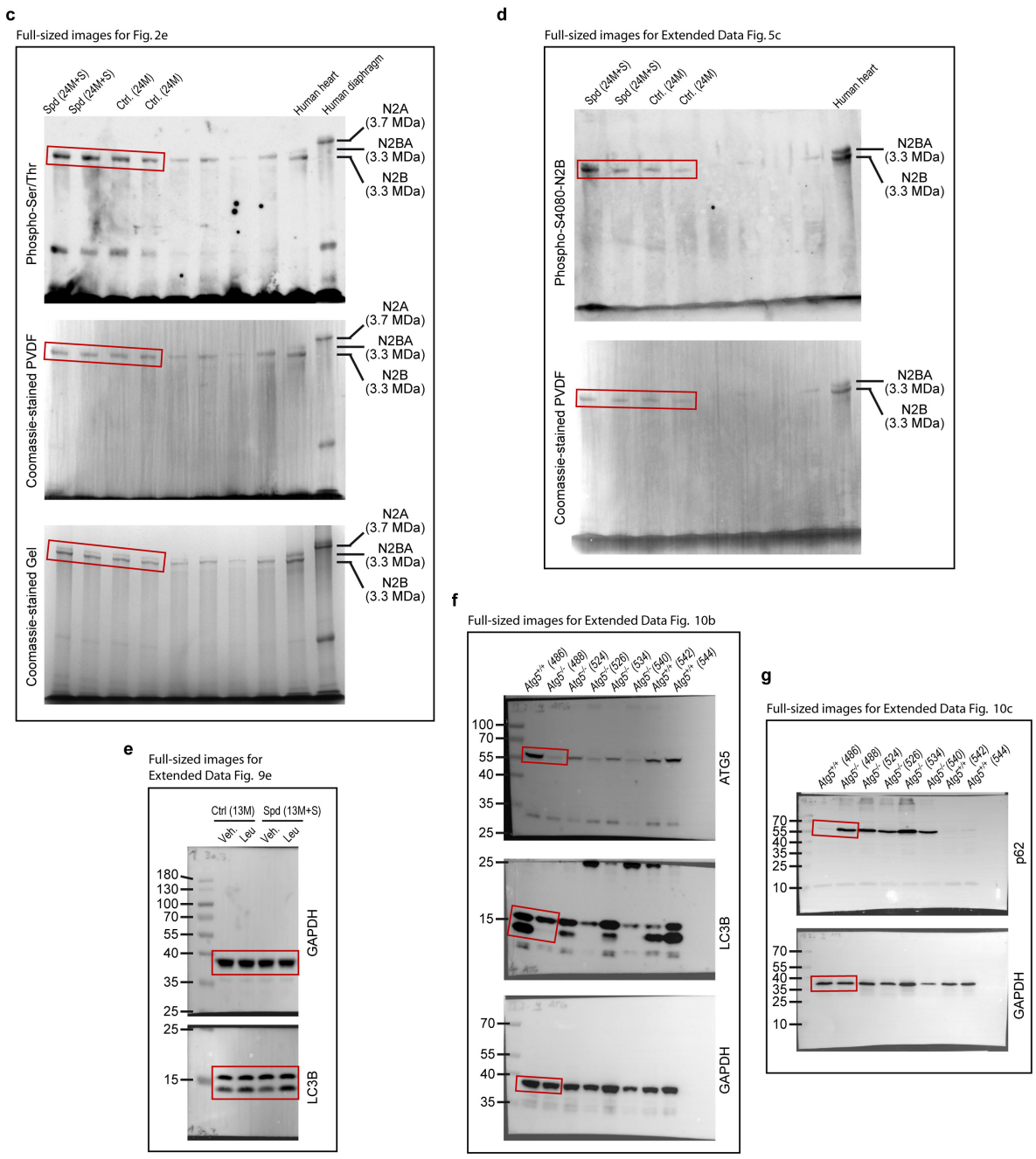

Supplementary Figure 18. Full-scans of western blots, membranes and gels.

Red boxes highlight areas that were cropped and shown in the indicated Figures.

Supplementary Table 1:

Number of mice included in lifespan experiments.

Total number of mice used for lifespan experiments as well as details on the number of sacrificed animals that were either included in the survival analyses (i.e. estimated deaths based on the *end-of-life* criteria defined in Methods) or censored due to severe bite wounds, wounds after excessive grooming or ulcerative dermatitis.

					Animal numbers			
Aging cohort	**Mouse strain**	**Sex**	**Treatment strategy**	**Treatment group**	**Total**	**Natural deaths**	**Estimated deaths**	**Censored**
1	C57BL/6J:Crl[1]	Female	*Life-long* treatment	Control	40	14	9	17
				Spermidine	41	17	3	21
				Spermine	17	13	2	2
				Putrescine	20	14	1	5
2	C57BL/6J[2]	Male & Female	*Late-in-life* treatment	Control	91	69	9	13
				Spermidine	87	64	5	18

[1]Obtained from Charles River Laboratories

[2]Obtained from our *in-house* animal facility (see Methods)

Supplementary Table 2:

Lifespan estimates and quartiles

Lifespan estimates and quartiles of the aging experiments presented in Fig. 1b-d.

			Lifespan estimates & quartiles			
Aging cohort	**Treatment strategy**	**Treatment group**	**Mean** (± s.e.m.)	**25%** (95% CI)	**50%** (95% CI) (*Median lifespan*)	**75%** (95% CI)
1	*Life-long* treatment	Control	796 ± 22	738 (680/768)	801 (746/859)	869 (807/933)
		Spermidine	880 ± 24	820 (700/896)	899 (834/966)	955 (899/1009)
		Spermine	892 ± 28	787 (757/913)	913 (801/955)	955 (927/1047)
		Putrescine	815 ± 35	717 (647/822)	822 (722/886)	926 (822/1005)
2	*Late-in-life* treatment	Control	769 (± 17)	663 (637/695)	770 (723/827)	889 (835/916)
		Spermidine	819 (±16)	729 (705/769)	847 (792/887)	922 (895/958)

Supplementary Table 3:

Advanced Age (28-month-old mice) Pathology

Tissue pathology and assessment of tumor incidence and severity in *life-long* spermidine-treated 28-month-old mice (28M+S) at the indicated concentrations of spermidine (in drinking water) compared to age-matched controls (28M) or young adult mice (5M).

		Tissue pathology							Cardiac pathology	
Animal	**Group[#]**	**Liver**	**Kidney**	**Spleen**	**Brain**	**Lung**	**Others**	**Tumor severity[$]**	**Abnorm-alities**	**Estimated area**
1	5M	microgranuloma, lipofuscine	NAD	siderosis	NAD	NAD			NAD	0
2	5M	microgranuloma, lipofuscine	protein casts	NAD	NAD	NAD			NAD	0
3	5M	NAD	NAD	NAD	NAD	NAD			NAD	0
4	5M	NAD	NAD	NAD	NAD	NAD			NAD	0
5	5M	microgranuloma	NAD	NAD	NAD	NAD			NAD	0
6	5M	microgranuloma	NAD	NAD	slight meningitis	NAD			NAD	0
7	5M	NAD	NAD	NAD	slight meningitis	NAD			small infarct	<1%
8	5M	NAD	NAD	NAD	NAD	NAD			NAD	0
9	5M	microgranuloma	NAD	siderosis	NAD	NAD			NAD	0
10	28M	NAD	protein casts	siderosis	slight encephalitis	NAD	histiocytic sarcoma	m	NAD	0
11	28M	microgranuloma	cyst, KALT	siderosis	NAD	BALT	pituitary adenoma, apoplex	m	NAD	0
12	28M	steatosis, microgranuloma	chronic nephritis, scars	NAD	NAD	BALT	pituitary adenoma	b	NAD	0
13	28M	microgranuloma, lipofuscine	NAD	histiocytic sarcoma				m + s	small cardiomyocyte degeneration, histiocytic sarcoma	~1%
14	28M	microgranuloma, lipofuscine	lymphoma	siderosis	NAD	lymphoma		m + s	NAD	0
15	28M	microgranuloma	protein casts	siderosis	NAD	BALT,	pituitary adenoma, pheochromocytoma, follicular call adenoma thyroid	b;b;b	NAD	0

16	28M	microgranuloma, steatosis	NAD	siderosis	NAD	lymphoma	pituitary carcinoma	m + s; m	NAD	0
17	28M	lymphoma	lymphoma	lymphoma	NAD	lymphoma		m + s	NAD	0
27	28M+S (0.3 mM)	histiocytic sarcoma, mulifocal livercell necrosis	chronic nephritis, scars	histiocytic sarcoma	NAD	histiocytic sarcoma, bronchioalveolar adenoma		m + s		0
28	28M+S (0.3 mM)	NAD	KALT	siderosis	NAD	BALT, pneumonia	pituitary adenoma	b	NAD	0
29	28M+S (0.3 mM)	NAD	NAD	NAD	NAD	BALT	pituitary adenoma, apoplex, follicular call adenoma thyroid	m	NAD	0
18	28M+S (3 mM)	histiocytic sarcoma, mulifocal livercell necrosis	histiocytic sarcoma	histiocytic sarcoma	NAD	histiocytic sarcoma	pituitary adenoma	m + s	histiocytic sarcoma	~3%
19	28M+S (3 mM)	Polyploidy	lymphoma	siderosis	meningeosis leukaemica	lymphoma	pituitary adenoma	s; b	NAD	0
20	28M+S (3 mM)	histiocytic sarcoma, mulifocal livercell necrosis	histiocytic sarcoma, tumorthrombi	histiocytic sarcoma	histiocytic sarcoma	histiocytic sarcoma, tumorthrombi	pituitary adenoma	m + s	tumorthrombi	<1%
21	28M+S (3 mM)	histiocytic sarcoma, amyloidosis	histiocytic sarcoma, amyloidosis	histiocytic sarcoma, amyloidosis	NAD	histiocytic sarcoma	pituitary adenoma	m + s	amyloidosis	<1%
22	28M+S (3 mM)	histiocytic sarcoma	histiocytic sarcoma	histiocytic sarcoma	NAD	NAD		m + s	NAD	0
23	28M+S (3 mM)	microgranuloma, lipofuscine	protein casts	siderosis	hydrocephalus	local pneumonia	pheochromocytoma, pituitary carcinoma	m	small infarct base	~2%
24	28M+S (3 mM)	amyloidosis	amyloidosis, chronic nephritis	amyloidosis	NAD	amyloidosis			amyloidosis, multiple small infarcts	~5%
25	28M+S (3 mM)	microgranuloma	NAD	siderosis	NAD	BALT,	histiocytic sarcoma, pituitary adenoma, pheochromocytoma	m; b	NAD	0
26	28M+S (3 mM)	steatosis	NAD	siderosis	NAD	BALT,	pituitary adenoma	b	NAD	0

[#] Age at necropsy in months (M). Compare also to Fig. 1a: 5M, young controls; 28M, aged controls; 28M+S, aged spermidine-treated. Spermidine was supplemented to drinking water starting from the age of 5 months (*life-long* treatment) at the indicated concentrations.

[$] According to “WHO International Classification of Rodent Tumors” (Ref. 89).

Abbreviations used: NAD, no abnormalities detected; LALT, liver-associated lymphatic tissue; KALT, kidney-associated lymphatic tissue; BALT, bronchus-associated lymphatic tissue

Supplementary Table 4:

End-of-life (EOL) animal necropsy

Tissue pathology and assessment of tumor incidence and severity as well as cause of death estimation in *end-of-life* animals identified to be close to their natural death due to aging and therefore euthanized (refer to methods for details).

			Tissue pathology							Cardiac pathology				
EOL animal	**Group**	**Age at necropsy (days)**	**Liver**	**Kidney**	**Spleen**	**Brain**	**Lung**	**Others**	**Tumor severity$**	**Abnorm-alities**	**Estimated area**	**Cleaved Caspase-3 pos. area**	**Cardiac death probable?**	**Most-likely cause of death**
1	Control	696	polyploidy, parenchyma atrophy	KALT, tubule epithelia regenerate, scars, protein casts	lymphatic hyperplasia	processing artefacts (vacuoles)	bronchioalveolar adenocarcinoma		m	NAD	0	0	no	n.d.
2	Control	704	microgranuloma	tubule epithelia regenerate, protein casts	lymphatic hyperplasia	processing artefacts (vacuoles)	NAD	histiocytic sarcoma	m	NAD	0	0	no	MODS
3	Control	508	histiocytic sarcoma	tubule epithelia regenerate,	histiocytic sarcoma	NAD	NAD		m	NAD	0	0	no	MODS
4	Control	738	microgranuloma	protein casts	NAD	NAD	bronchioalveolar adenoma		b	NAD	0	< 1%	no	n.d.
5	Control	747	histiocytic sarcoma, infarcts, congestion, LALT	histiocytic sarcoma	histiocytic sarcoma, congestion	NAD	histiocytic sarcoma		m & s	NAD	0	>1% < 3%	no	Liver failure
6	Control	750	LALT	chronic nephritis, tubule epithelia regenerate, cysts	NAD	processing artefacts (vacuoles)	BALT		0	NAD	0	< 1%	no	kidney failure
7	Control	768	bilary duct carcinoma, inflammation	Glomerular sclerosis, tubule epithelia regenerates, protein casts	Lymphoma	NAD	NAD		m & s	NAD	0	0	no	MODS
8	Control	801	Lymphoma	Lymphoma	Lymphoma	NAD	Lymphoma		s	NAD	0	< 1%	no	MODS
9	Control	594	histiocytic sarcoma	histiocytic sarcoma	Lymphoma	Meningeosis leukaemia	Lymphoma		m & s	NAD	0	< 1%	no	MODS
10	Control	859	LALT, slight inflammation	small abscesses	Hyperplasia	meningitis, encephalitis	pneumonia		0	multiple infarcts	~5%	> 1% < 3%	no	MODS inf.
11	Control	658	hepatocellular carcinoma	slight inflammation, tubule epithelia regenerate, scars	NAD	NAD	histiocytic sarcoma,		m & s	NAD	0	> 1% < 3%	no	MODS
12	Control	869	Lymphoma	Lymphoma, infarcts, glomerulosclerosis	Lymphoma	eosinophilic thalamic inclusions	Lymphoma, Thrombi		m & s	NAD	0	> 1% < 3%	no	MODS

13	Control	647	mild amyloidosis	mild amyloidosis	mild amyloidosis, siderosis	pituitary adenoma, hydro-cephalus	atelectasis, aspi. Hair		0	small myocardial infarcts	~1%	< 1%	no	lung failure
14	Control	714	mild activation of Kuppfer cells	tubule epithelia regenerates, scars	lymphatic hyperplasia	NAD	lymphatic infiltrates in septae, infarcts		0	perivascular fibrosis, myxoid valves	~2%, ~5%	> 2% < 5%	no	MODS inf.
15	Control	737	Lymphoma	infarcts, subcapsular lymphoma infiltrates	Lymphoma	processing artefacts (vacuoles)	Lymphoma, congestion	LN with central necrosis	m & s	small myocardial infarcts	~3%	> 2% < 5%	no	MODS
16	Control	758	mild activation of Kuppfer cells, microgranuloma	subcapsular lymphoma infiltrates	Lymphoma	slight encephalitis	subpleural lymphoma infiltrates		m & s	small myocardial infarcts + intramural infiltrates	~1%; ~5%	< 1%	no	MODS
17	Control	758	histiocytic sarcoma,	histiocytic sarcoma, cysts	histiocytic sarcoma,	NAD	histiocytic sarcoma,		m & s	NAD	0	0	no	MODS
18	Control	805	Lymphoma, cholestasis	Lymphoma	Lymphoma, Siderosis	slight encephalitis	bronchioalveolar carcinoma with osseos metaplasia		m & s	perivascular fibrosis	~1%	< 1%	no	MODS
19	0.3 mM Spd	696	histiocytic sarcoma, atrophic parenchyma	histiocytic sarcoma	lymphatic hyperplasia	processing artefacts (vacuoles)	histiocytic sarcoma		m & s	NAD	0	< 1%	no	MODS
20	0.3 mM Spd	768	NAD	KALT	lymphatic hyperplasia, starry sky	NAD	papillary bronchioalveolar carcinoma		m	NAD	0	< 1%	no	lung failure
21	0.3 mM Spd	820	bilary duct carcinoma, inflammation	protein casts, KALT	NAD	processing artefacts (vacuoles)	NAD		m & s	NAD	0	> 1% < 3%	no	MODS
22	0.3 mM Spd	869	inflammation, infarcts	chronic nephritis, tubule epithelia regenerate	lymphatic hyperplasia, starry sky	slight encephalitis	congestion, inflammation		0	small infarcts at septum,	~1%	> 1% < 3%	no	MODS inf.
23	0.3 mM Spd	675	Hepatitis	slight nephritis,	lymphatic hyperplasia, starry sky	processing artefacts (vacuoles)	bronchioalveolar carcinoma		m	intramural inflammation	~3%	> 1% < 3%	no	lung failure
24	0.3 mM Spd	696	inflammatory infiltrates, mild amyloidosis	chronic nephritis, tubule epithelia regenerate, scars, mild amyloidosis	Lymphoid hyperplasia, Amyloidosis	processing artefacts (vacuoles)	infarcts	sialadenitis, ulcer, histiocytic granuloma	0	small myocardial infarcts, fibrosis,hyper trophy	~1%; ~3%; 30%	> 1% < 3%	no	MODS inf.
25	0.3 mM Spd	716	centrolobular necrosis, Kuppfer cell acticvation	tubule epithelia regenerates, KALT	lymphatic hyperplasia	processing artefacts (vacuoles)	lymphatic infiltrates in septae	genital squamous cell carcinoma, bladderthro mbus	m	hypertrophy	30%	> 1% < 3%	no	MODS inf.

26	3 mM Spd	479	hepatocellular carcinoma, polyploidy, microgranuloma	chronic nephritis, tubule epithelia regenerate, scars	lymphatic hyperplasia	purulent meningitits	granulocyte cluster infiltrates (metastatic pneumonia)	histiocytic sarcoma	m & s	NAD	0	0	no	MODS
27	3 mM Spd	704	slight vacuolation	KALT	NAD	NAD	NAD		0	NAD	0	< 1%	no	n.d.
28	3 mM Spd	715	histiocytic sarcoma,	protein casts	histiocytic sarcoma	NAD	histiocytic sarcoma		m & s	NAD	0	0	no	MODS
29	3 mM Spd	738	atrophic parenchyma, microgranuloma	tubule epithelia regenerate, protein casts	lymphatic hyperplasia	NAD	hemosiderosis, bleeding		0	small myocardial infarct	~1%	< 1%	no	n.d.
30	3 mM Spd	738	histiocytic sarcoma	tubule epithelia regenerate	histiocytic sarcoma	processing artefacts (vacuoles)	histiocytic sarcoma		m & s	NAD	0	0	no	MODS
31	3 mM Spd	747	hepatocellular carcinoma, polyploidy, microgranuloma	tubule epithelia regenerate, protein casts	Lymphoma	processing artefacts (vacuoles)	NAD		m & s	Hypertrophy	50%	> 2% < 5%	no	MODS
32	3 mM Spd	587	Lymphoma, Amyloidosis	Lymphoma, Amyloidosis	Lymphoma, Amyloidosis	NAD	Lymphoma, Amyloidosis		m & s	NAD	0	0	no	MODS due to amyloid
33	3 mM Spd	801	inflammation, LALT	inflammation, KALT	lymphatic hyperplasia, starry sky	processing artefacts (vacuoles)	NAD		0	NAD	0	< 1%	no	MODS inf.
34	3 mM Spd	637	histiocytic sarcoma,	histiocytic sarcoma, tumorthrombi, infarcts	histiocytic sarcoma,	hydro-cephalus	tumorthrombi		m & s	Hypertrophy	30%	> 2% < 5%	no	MODS
35	3 mM Spd	647	microgranuloma, polyploidy	chronic nephritis, tubule epithelia regenerate, protein casts, scars	lymphatic hyperplasia, starry sky	processing artefacts (vacuoles)	congestion, histiocytic infiltrates, bronchioalveolar carcinoma		m	hypertrophy	30%	0	no	lung failure
36	3 mM Spd	703	Lymphoma	tubule epithelia regenerate, subcapsular lymphoma infiltrates	Lymphoma	Meningeosis leukaemia	Lymphoma		m & s	perivascular fibrosis	~1%	> 1% < 3%	no	MODS
37	3 mM Spd	714	cholangiofibrosis, lymphoma, infarcts	lymphoma, tumorthrombi, infarcts	Lymphoma	processing artefacts (vacuoles)	Lymphoma, infarcts		m & s	Dilation	20-30%	< 1%	no	MODS
38	3 mM Spd	779	slight inflammation, cholestasis	Congestion	NAD	pituitary adenoma, hydrocephalus	NAD	Fibrosarcoma	m	small myocardial infarcts	~3%	> 1% < 3%	no	MODS

[$] According to “WHO International Classification of Rodent Tumors” (Ref. 89).

Abbreviations used: NAD, no abnormalities detected; LALT, liver-associated lymphatic tissue; KALT, kidney-associated lymphatic tissue; MODS, multiple-organ dysfunction; MODS inf., MODS due to generalized inflammation.

Supplementary Table 5:

Left ventricular echocardiographic parameters of C57BL/6J aging mice.
Young (4M), middle-aged (18M) and aged (23M) controls were compared with aged *late-in-life* spermidine-treated (23M+S) C57BL/6J male mice (see Fig. 1a for the feeding scheme). Abbreviations: EF, ejection fraction; FS, fractional shortening; HR, heart rate; IVS, interventricular septum thickness during diastole; LV, left ventricular; LVEDD, left ventricular end-diastolic diameter; LVESD, left ventricular end-systolic diameter; PW, posterior wall thickness during diastole; RWT, relative wall thickness; TL, tibia length. Data show means ± s.e.m. of indicated number of mice analysed per group.

	Young	**Aged**		
	(4M) N=10	**(18M) N=14**	**(23M) N=20**	**(23M+S) N=20**
Body weight (g)	25.1±0.5***	33.9±0.8***	30±0.6	30.2±0.6
HR (bpm)	572±18	545±16	538±13	519±17
LV mass (mg)	92±3***	152±6	153±6	137±4§
LV mass/TL (mg/mm)	5.17±0.17***	8.48±0.35	8.73±0.37	7.52±0.22*
IVS (mm)	0.80±0.02***	1.04±0.03	1.05±0.03	0.99±0.03
IVS/TL	0.045±0.001***	0.058±0.001	0.06±0.002	0.055±0.002
PW (mm)	0.73±0.02***	0.89±0.02	0.94±0.03	0.86±0.02§
PW/TL	0.041±0.001***	0.05±0.001	0.054±0.002	0.047±0.001**
LVEDD (mm)	3.57±0.05**	3.99±0.06	3.88±0.06	3.88±0.05
LVESD (mm)	2.00±0.10*	2.52±0.07	2.33±0.08	2.26±0.07
RWT	0.43±0.01**	0.48±0.01	0.52±0.02	0.48±0.01
FS (%)	44±2	37±1	40±1	42±1
EF (%)	76±2	67±2	71±2	73±1

***p<0.001, **p<0.01, *p<0.05 *vs.* 23M (ANOVA with post-hoc Tukey or Welch's test with post-hoc Games-Howell according to equality of variances)
§p<0.05 *vs.* 23M (unpaired Student's *t*-test comparing 23M+S *vs.* 23M)

Supplementary Table 6:

Left ventricular hemodynamic parameters of C57BL/6J aging mice.
Young (4M), middle-aged (18M) and aged (24M) controls were compared with aged *late-in-life* spermidine-treated (24M+S) C57BL/6J male mice (see Fig. 1a for the feeding schemes). Abbreviations: CO, cardiac output; dP/dt_{max}, peak rate of pressure rise; dP/dt_{min}, peak rate of pressure decay; Ea, arterial elastance; EF, ejection fraction; ESP, end-systolic pressure; EDP, end-diastolic pressure; ESV, end-systolic volume; EDV, end-diastolic volume; HR, heart rate; P_{max}, maximum ventricular pressure; SV, stroke volume; τ, left ventricular pressure decay time constant (according to Weiss' Method); VVC, ventricular-vascular coupling; EDPVR β, Exponential end-diastolic pressure-volume relationship chamber stiffness constant; ESPVR Ees, Linear end-systolic pressure-volume relationship slope. Data show means ± s.e.m. or median [IQR] (according to normality) of indicated number of mice analyzed per group.

	Young	**Aged**		
	(4M) N=10	**(18M) N=8**	**(24M) N=10**	**(24M+S) N=10**
HR (bpm)	505±10*	502±20	457±12	476±26
EF (%)	76±3	66±2	70±1	71±2
CO (ml/min)	20.8 [20.4-21]	23 [20.8-26.1]	20.2 [19.6-23.4]	23.9 [20.6-25]
SV (µl)	40.4±0.9**	45.2±1.7	47±1.1	48.1±1.5
ESV (µl)	12.9±1.6**	24.1±2.2	20.9±1.5	20.1±1.6
EDV (µl)	53.3±1.6***	69.3±2.8	67.8±2.3	68.2±2.1
P_{max} (mmHg)	68±2*	69±3	56±3	59±5
ESP (mmHg)	56±2	61±2	50±3	50±4
EDP (mmHg)	3.3±0.4$^{\#}$	4.6±0.3	5.2±0.7	3.3±0.5$^{\#}$
Ea (mmHg/µl)	1.39±0.06**	1.37±0.06*	1.06±0.06	1.06±0.09
dP/dt_{max} (mmHg/s)	3298±130	3825±332*	2580±261	3131±381
dP/dt_{min} (mmHg/s)	-3445±177$^{\#}$	-3528±291*	-2396±255	-2803±372
τ (ms)	6.9±0.3*	7.7±0.7	10.6±1.3	8.1±0.8§
VVC	1.45±0.18	1.07±0.17	1.02±0.1	1.63±0.19*
ESPVR Ees (mmHg/µl)	2.05±0.31*	1.51±0.26	1.06±0.1	1.76±0.28
EDPVR β (µl)	0.023±0.004*	0.025±0.004	0.049±0.009	0.031±0.003**

***p<0.001, **p<0.01, *p<0.05, $^{\#}$p<0.055 *vs.* 24M (ANOVA with post-hoc Tukey, Welch's test with post-hoc Games-Howell or Kruskal-Wallis followed by corrected multiple comparisons by Mann-Whitney U-test according to normality and equality of variances. For details, please refer to Methods section). §p<0.05 *vs.* 24M (unpaired Student's *t*-test comparing 24M+S *vs.* 24M)
Note: for ESPVR Ees and EDPVR β, other parameters in the fitting equation (V_0 and α, respectively) were included as covariates using ANCOVA and post-hocs were Bonferroni-corrected.

Supplementary Table 7:

Gravimetric analysis of C57BL/6J aging mice.
Young (4M), middle-aged (18M) and aged (24M) controls were compared with aged *late-in-life* spermidine-treated (24M+S) C57BL/6J male mice (see Fig. 1a for the feeding scheme). Abbreviations: BAT, brown adipose tissue; WAT, white adipose tissue; TL, tibia length. Data show means ± s.e.m. of indicated number of mice analyzed per group.

	Young	Aged		
	(4M) N=10	(18M) N=8	(24M) N=10	(24M+S) N=10
Body weight (g)	28.2±0.6	35.1±1**	30.6±1	29.3±0.7
Heart weight (HW, mg)	136±6***	194±10	200±12	191±9
HW/TL (mg/mm)	7.7±0.4***	10.9±0.6	11.2±0.7	10.8±0.5
Lung weight (mg)	157±4**	168±8	187±3	166±6*
Lung weight/TL (mg/mm)	8.8±0.3**	9.4±0.5	10.5±0.2	9.4±0.3§
Kidney weight (mg)	336±11	433±5***	279±21	295±25
Kidney weight/TL (mg/mm)	18.9±0.8	24.3±0.4***	15.7±1.3	16.8±1.5
Liver weight (mg)	1376±82*	1606±114	1688±82	1651±65
Liver weight/TL (mg/mm)	77.7±5.1	90.4±6.9	94.3±4.2	93.5±3.4
Spleen weight (mg)	80±8***	102±8	156±19	159±16
WAT (mg)	347±33**	1057±185**	165±16	177±14
BAT (mg)	64±2	85±11	59±7	50±5

***p<0.001, **p<0.01, *p<0.05 *vs.* 24M (ANOVA with post-hoc Tukey or Welch's test with post-hoc Games-Howell according to equality of variances)
§p<0.05 *vs.* 24M (unpaired Student's *t*-test comparing 24M+S *vs.* 24M)

Supplementary Table 8:

Left ventricular morphology of C57BL/6J aging mice.
Young (4M) and aged (24M) controls were compared with aged *late-in-life* spermidine-treated (24M+S) C57BL/6J male mice (see Fig. 1a for the feeding scheme) using design-based stereology. Data show means ± s.d. of indicated number of mice analyzed per group. **V_V(structure/reference volume)**, relative volumes calculated as the fractions of indicated reference volumes. **V(structure, volume),** absolute volumes given in mm^3. Abbreviations used: myo, myocytes; lv, left ventricle; int, interstitium; coll, collagen; lum, vessel lumina; wall, vessel wall; lg, lipofuscin granules; nuc, nuclei; mf, myofibrils; mi, mitochondria; sp, (mitochondria- and myofibril-free) sarcoplasm.

	Young	Aged	
	(4M) N=10	**(24M) N=15**	**(24M+S) N=14-15**
V_V(myo/lv)	0.873±0.034***	0.762±0.069	0.752±0.058
V_V(int/lv)	0.127±0.034***	0.238±0.069	0.248±0.058
V(myo,lv)	71.2±6.25*	86.3±16.7	87.4±10.3
V(int,lv)	10.3±2.56***	26.8±8.6	29.1±8.6
V_V(coll/int)	0.006 [0.005-0.007]	0.013 [0.007-0.017]	0.02 [0.008-0.025]
V_V(lum/int)	0.284 [0.259-0.309]	0.238 [0.187-0.281]	0.206 [0.185-0.251]
V_V(wall/lv)	0.199±0.048	0.104±0.028	0.119±0.022
V(coll,lv)	0.069±0.038**	0.339±0.267	0.501±0.328
V(lum,lv)	2.97±1.20**	6.34±2.85	6.35±1.62
V(wall,lv)	1.91 [1.71-2.23]*	2.4 [2.15-2.96]	3.4 [2.74-3.77]*
V_V(lg/myo) [*10^{-3}]	*0.041±0.086*†	0.807±0.424	1.190±0.919
V(lg,lv)	*0.003±0.006*†	0.070±0.039	0.105±0.083
V_V(nuc/myo)	0.021±0.005	0.022±0.008	0.021±0.007
V_V(mf/myo)	0.543±0.023*	0.505±0.039	0.554±0.038***
V_V(mi/myo)	0.347±0.015***	0.276±0.028	0.325±0.024***
V_V(sp/myo)	0.088±0.010***	0.197±0.054	0.099±0.027***
V(nuc,lv)	1.52±0.37	1.83±0.645	1.87±0.68
V(mf,lv)	38.7±4.46	43.5±8.66	48.3±5.47
V(mi,lv)	24.7±2.04	23.6±3.85	28.5±4.33**
V(sp,lv)	6.27 [5.77-6.7]***	17.29 [13.53-18.13]	8.39 [6.88-10.48]***

†*Note that lipofuscin granules (lg) were only detectable in 2 out of 10 young (4M) subjects, rendering this data impossible to analyze by general linear statistical models. Therefore, the aged groups (24M vs. 24M+S) were compared by Students t-test yielding no significant differences.*

***p<0.001, **p<0.01, *p<0.05 *vs.* 24M (ANOVA with post-hoc Tukey, Welch's test with post-hoc Games-Howell or Kruskal-Wallis followed by corrected multiple comparisons by Mann-Whitney U-test according to normality and equality of variances. For details, please refer to Methods section).

Supplementary Table 9:

Functional classification of cardiac tissue protein abundance affected by spermidine. Spermidine was supplemented *late-in-life* to aging C57BL/6J male mice until age 24M (see Fig. 1a for the feeding scheme) and cardiac proteomic profiles from spermidine-fed animals were compared with age-matched controls (compare Supplementary Fig. 6b). Over-represented gene ontology (GO) terms ($p<0.05$ uncorrected, selected GO's are presented) were identified by *PANTHER*[90] (release 20150430).

GO (category)	Genes
Complement activation (BP)	C4b, Serping1, C3, C5
Myosin filament (CC)	Myh6/7, Myh4, Myh10, Myh11
Mitochondrial respiratory chain complex I (CC)	Ndufb5, Ndufb7, Ndufb8, Ndufb9, Ndufs3, Ndufs6

Supplementary Table 10:

Functional classification of differentially expressed genes in cardiac tissue by spermidine. Spermidine was supplemented *life-long* to aging female mice (see Fig. 1a for the feeding scheme) until age 30-32 month and cardiac transcriptomic profiles from spermidine-fed animals were compared with age-matched controls (compare Supplementary Fig. 6a). Over-represented gene ontology (GO) terms were identified by Ingenuity Pathway Analysis (IPA).

GO	Genes
Infection of mammalia	Cd274, Cxcl10, Igtp, Iigp1, Irgm, Stat1
Leukocyte migration	Cd274, Cxcl10, Defb8, Fgf2, Irgm, Serpina1, Stat1, Tfpi
Cell movement	Cap1, Cxcl10, Defb8, Fgf2, Gfra1, Golga2, Irgm, Ldhc, Serpina1, Stat1, Tfpi
Cellular homeostasis	Aga, Aspscr1, Cd274, Fgf2, Igtp, Iigp1, Irgm, Serpina1, Stat1

Supplementary Table 11:

Left ventricular echocardiographic parameters of Atg5-transgenic mice.
Control and spermidine-treated *Atg5$^{flox/flox}$/MLC2a-Cre^{-} (Atg5$^{+/+}$)* and *Atg5$^{flox/flox}$/MLC2a-Cre^{+} (Atg5$^{-/-}$)* male mice at the age of 13-14 weeks were used (see Supplementary Fig. 10a for the feeding scheme). Abbreviations: EF, ejection fraction; FS, fractional shortening; HR, heart rate; IVS, interventricular septum thickness during diastole; LV, left ventricular; LVEDD, left ventricular end-diastolic diameter; LVESD, left ventricular end-systolic diameter; PW, posterior wall thickness during diastole; RWT, relative wall thickness; TL, tibia length. Data show means ± s.e.m. of indicated number of mice analyzed per group.

	Atg5$^{+/+}$		***Atg5$^{-/-}$***		**Two-way ANOVA** (p-values)		
	Control (N=16)	Spermidine (N=15)	Control (N=12)	Spermidine (N=14)	Geno-type	Treat-ment	Inter-action
Body weight (g)	26.8±0.6	26.8±0.5	25.4±0.7	27.7±0.6*	n.s.	0.052	n.s.
HR (bpm)	558±14	567±13	535±9	559±16	n.s.	n.s.	n.s.
LV mass (mg)	116±5	104±3	121±5	139±8$^{+++,\ *}$	0.001	n.s.	0.008
LV mass/ TL (mg/mm)	6.65±0.29	5.84±0.17*	6.86±0.3	7.94±0.43$^{+++,\ *}$	<0.001	n.s.	0.004
IVS (mm)	0.87±0.02	0.86±0.02	0.86±0.03	0.97±0.03$^{++,\ **}$	0.055	n.s.	0.016
IVS/TL	0.05±0.001	0.05±0.001	0.05±0.002	0.06±0.002$^{++,\ *}$	0.03	n.s.	0.007
PW (mm)	0.81±0.02	0.76±0.02	0.83±0.02	0.89±0.02^{+++}	<0.001	n.s.	0.013
PW/TL	0.05±0.001	0.04±0.001*	0.05±0.001	0.05±0.002$^{+++,\ *}$	<0.001	n.s.	0.002
LVEDD (mm)	3.8±0.05	3.67±0.04	3.87±0.08	3.84±0.06^{+}	0.004	n.s.	n.s.
LVESD (mm)	2.22±0.09	2.08±0.06	2.34±0.08	2.43±0.08^{++}	0.005	n.s.	n.s.
RWT	0.78±0.04	0.79±0.03	0.74±0.03	0.78±0.03	n.s.	n.s.	n.s.
FS (%)	41.7±1.7	43.5±1.2	39.6±1.2	37±1.1^{++}	0.003	n.s.	n.s.
EF (%)	73±2	75±2	71±1	67±2^{++}	0.005	n.s.	n.s.

***p<0.001, **p<0.01, *p<0.05 *vs.* respective genotype-matched control (Simple main effects following significant two-way ANOVA)

$^{+++}$p<0.001, $^{++}$p<0.01, $^{+}$p<0.05 *vs.* respective treatment-matched *Atg5$^{+/+}$* (Simple main effects following significant two-way ANOVA)

Supplementary Table 12:

Left ventricular hemodynamic parameters of Atg5-transgenic mice.
Control and spermidine-treated *Atg5$^{flox/flox}$/MLC2a-Cre^{-}* (*Atg5$^{+/+}$*) and *Atg5$^{flox/flox}$/MLC2a-Cre^{+}* (*Atg5$^{-/-}$*) male mice at the age of 16 weeks were used (see Supplementary Fig. 10a for the feeding scheme). Abbreviations: CO, cardiac output; dP/dt_{max}, peak rate of pressure rise; dP/dt_{min}, peak rate of pressure decay; Ea, arterial elastance; EF, ejection fraction; ESP, end-systolic pressure; EDP, end-diastolic pressure; ESV, end-systolic volume; EDV, end-diastolic volume; HR, heart rate; P_{max}, maximum ventricular pressure; SV, stroke volume; τ, left ventricular pressure decay time constant (according to Weiss' Method); VVC, ventricular-vascular coupling; EDPVR β, Exponential end-diastolic pressure-volume relationship chamber stiffness constant; ESPVR Ees, Linear end-systolic pressure-volume relationship slope. Data show means ± s.e.m. of indicated number of mice analyzed per group.

	Atg5$^{+/+}$		***Atg5$^{-/-}$***		**Two-way ANOVA** (p-values)		
	Control (N=10)	Spermidine (N=10)	Control (N=9)	Spermidine (N=11)	Geno-type	Treat-ment	Inter-action
HR (bpm)	477±12	472±16	464±7	464±12	n.s.	n.s.	n.s.
EF (%)	76±2	76±1	74±1	70±1$^{+++,*}$	0.002	n.s.	0.051
CO (ml/min)	21±0.7	20.2±1.1	20.5±0.7	19.4±0.6	n.s.	n.s.	n.s.
SV (µl)	44.1±1.1	42.8±1.3	44.3±1.7	41.8±0.6	n.s.	n.s.	n.s.
ESV (µl)	14.3±1.4	13.2±0.4	15.3±0.8	18.4±1$^{+++,*}$	0.004	n.s.	0.045
EDV (µl)	58.4±2	56±1.5	59.7±1.6	60.2±1.2	n.s.	n.s.	n.s.
P_{max}	73±3	74±4	74±6	81±1	n.s.	n.s.	n.s.
ESP (mmHg)	60±3	64±4	65±6	70±2	n.s.	n.s.	n.s.
EDP (mmHg)	4.4±0.7	4.3±0.5	4.6±1.1	5.1±0.5	n.s.	n.s.	n.s.
Ea (mm Hg/µl)	1.38±0.07	1.51±0.11	1.46±0.13	1.68±0.05	n.s.	n.s.	n.s.
dP/dt_{max} (mmHg/s)	4048±398	4331±450	4371±688	4798±462	n.s.	n.s.	n.s.
dP/dt_{min} (mmHg/s)	-3787±308	-4085±417	-3913±554	-4445±309	n.s.	n.s.	n.s.
τ (ms)	6.8±0.3	7.4±0.4	8.1±0.8	6.9±0.4	n.s.	n.s.	n.s.
VVC	1.18±0.23	1.63±0.23*	0.83±0.1	0.81±0.05^{+++}	0.002	n.s.	n.s.
ESPVR Ees (mmHg/µl)	1.63±0.30	2.33±0.27†	1.24±0.20	1.35±0.09^{+}	0.048	n.s.	n.s.
EDPVR β (µl)	0.020±0.002	0.020±0.002	0.021±0.003	0.039±0.005*	n.s.	n.s.	0.045

***p<0.001, **p<0.01, *p<0.05 and †p = 0.054 *vs.* respective genotype-matched control (Simple main effects following significant two-way ANOVA)
$^{+++}$p<0.001, $^{++}$p<0.01, $^{+}$p<0.05 *vs.* respective treatment-matched *Atg5$^{+/+}$* (Simple main effects following significant two-way ANOVA)
Note: for ESPVR Ees and EDPVR β, other parameters in the fitting equation (V_0 and α, respectively) were included as covariates using ANCOVA.

Supplementary Table 13:

Gravimetric analysis of Atg5-transgenic mice.

Control and spermidine-treated *Atg5*$^{flox/flox}$/*MLC2a-Cre*$^{-}$ (*Atg5*$^{+/+}$) and *Atg5*$^{flox/flox}$/*MLC2a-Cre*$^{+}$ (*Atg5*$^{-/-}$) male mice at the age of 16 weeks were used (see Supplementary Fig. 10a for the feeding scheme). Abbreviations: BAT, brown adipose tissue; WAT, white adipose tissue; TL, tibia length. Data show means ± s.e.m. of indicated number of mice analyzed per group.

	***Atg5*$^{+/+}$**		***Atg5*$^{-/-}$**		**Two-way ANOVA** (p-values)		
	Control (N=10)	Spermidine (N=10)	Control (N=9)	Spermidine (N=11)	Geno-type	Treat-ment	Inter-action
Body weight (g)	27.4±0.8	28.1±0.9	26.5±0.5	28.5±0.7	n.s.	n.s.	n.s.
Heart weight (HW, mg)	144±9	144±5	147±7	154±6	n.s.	n.s.	n.s.
HW/TL (mg/mm)	8.17±0.48	8.09±0.27	8.43±0.38	8.79±0.3	n.s.	n.s.	n.s.
Lung weight (mg)	144±8	154±6	144±7	160±6	n.s.	n.s.	n.s.
Lung weight/TL (mg/mm)	8.18±0.49	8.68±0.32	8.23±0.36	9.11±0.3	n.s.	n.s.	n.s.
Kidney weight (mg)	326±17	341±8	317±8	321±10	n.s.	n.s.	n.s.
Kidney weight/TL (mg/mm)	18.51±0.87	19.22±0.52	18.1±0.42	18.35±0.51	n.s.	n.s.	n.s.
Liver weight (g)	1268±76	1283±70	1194±37	1378±67	n.s.	n.s.	n.s.
Liver weight/TL (mg/mm)	71.98±3.82	71.2±3.7	68.29±2.13	78.68±3.74	n.s.	n.s.	n.s.
Spleen weight (mg)	77±6	79±6	69±2	75±5	n.s.	n.s.	n.s.
WAT (mg)	455±69	362±24	450±65	550±74	n.s.	n.s.	n.s.
BAT (mg)	63±5	68±6	62±11	68±6	n.s.	n.s.	n.s.

Supplementary Table 14:

Left ventricular echocardiographic parameters of *Dahl* salt-sensitive rats.
Control and spermidine-treated *Dahl* salt-sensitive rats fed a high-salt diet (8% NaCl) starting from the age of 7 weeks (see Fig. 4a for the feeding scheme) were used at the indicated ages. Abbreviations: E/E', peak early filling Doppler velocity of transmitral flow (E) to the corresponding myocardial tissue Doppler velocity (E') ratio; EF, ejection fraction; FS, fractional shortening; HR, heart rate; IVS, interventricular septum thickness during diastole; RWT, relative wall thickness; LA, left atrium; LV, left ventricular; LVEDD, left ventricular end-diastolic diameter; LVESD, left ventricular end-systolic diameter; PW, left ventricular posterior wall thickness during diastole. Data show means ± s.e.m. of indicated number of rats analyzed per group.

	9-week-old (2 weeks high-salt)		**14-week-old** (7 weeks high-salt)		**19-week-old** (12 weeks high-salt)		**Two-way ANOVA (p-values[§])**		
	Control (N=10)	Spermidine (N=10)	Control (N=10)	Spermidine (N=10)	Control (N=10)	Spermidine (N=10)	Age	Treatment	Interaction
Body weight (g)	300±4	268±3***	371±5^{+++}	341±5$^{***,\,+++}$	360±11^{+++}	389±11	<0.001	n.s.	<0.001
HR (bpm)	377±6	387±6	375±5	378±6	371±5	376±4	n.s.	n.s.	n.s.
LV mass (mg)	1304±29	1231±36	1762±66^{+++}	1404±44$^{***,\,+}$	2053±85^{+++}	1719±55$^{**,\,+++}$	<0.001	<0.001	0.02
LV mass/body weight (mg/g)	4.36±0.13	4.60±0.16	4.75±0.17	4.11±0.1$^{**,\,+}$	5.70±0.15^{+++}	4.43±0.14***	<0.001	<0.001	<0.001
LA area (mm^2)	22.3±1	21.8±0.9	27.9±0.8^{+++}	26.8±0.6^{+}	27.7±1.3^{++}	24.2±0.7*	<0.001	0.01	n.s.
IVS (mm)	2.20±0.04	2.09±0.04	2.74±0.07^{+++}	2.36±0.07$^{**,\,+}$	2.99±0.05^{+++}	2.69±0.09$^{*,\,+++}$	<0.001	<0.001	0.043
PW (mm)	2.38±0.06	2.25±0.07	2.73±0.08^{+++}	2.42±0.08*	3.12±0.13^{+++}	2.65±0.07$^{**,\,++}$	<0.001	0.003	0.048
LVEDD (mm)	7.10±0.1	7.14±0.1	7.30±0.15	7.33±0.11	7.26±0.19	7.39±0.13	0.035	n.s.	n.s.
LVESD (mm)	3.08±0.09	3.33±0.14	3.51±0.11^{+++}	3.60±0.13^{+}	4.26±0.16^{+++}	4.11±0.21^{+++}	<0.001	n.s.	n.s.
RWT	2.88±0.06	2.79±0.08	3.30±0.08^{+++}	3.02±0.07$^{*,\,+}$	3.41±0.07^{+++}	3.05±0.03$^{***,\,++}$	<0.001	0.002	n.s.
FS (%)	57±1	54±2	52±1^{++}	51±1	42±1^{+++}	45±2^{+++}	<0.001	n.s.	0.028
EF (%)	84±1	83±1	81±1	79±1^{+}	73±1^{+++}	76±1^{+++}	<0.001	n.s.	0.017
E/E'	22.4±1.4	24.4±1.2	35.2±1.6^{+++}	28.2±1.1$^{**,\,+++}$	43.9±1.4^{+++}	32.9±1.1$^{***,\,+++}$	<0.001	0.001	<0.001

[§]p-values of two-way ANOVA (mixed-design) including two factors: (i) age (9, 14 and 19 weeks, as repeated measurements) and (ii) treatment (high-salt control *vs.* high-salt + spermidine, as independent observations).
***p<0.001, **p<0.01, *p<0.05 *vs.* age-matched control (Simple main effects following significant two-way ANOVA)
$^{+++}$p<0.001, $^{++}$p<0.01, $^{+}$p<0.05 *vs.* 9-week-old treatment-matched group (Simple main effects [Bonferroni-corrected] following significant two-way ANOVA)

Supplementary Table 15:

Gravimetric analysis of *Dahl* salt-sensitive rats.

Control and spermidine-treated *Dahl* salt-sensitive rats fed a high-salt (8% NaCl) diet starting from the age of 7 weeks (see Fig. 4a for the feeding scheme) were used at the indicated ages. Abbreviations: TL, tibia length. Data show means ± s.e.m. of indicated number of rats analyzed per group.

	7-week-old (no high-salt)	**14-week-old (7 weeks high-salt)**		**19-week-old (12 weeks high-salt)**		**Two-way ANOVA** (p-values[§])		
	Control (N=10)	Control (N=9)	Spermidine (N=9)	Control (N=10)	Spermidine (N=10)	Age	Treatment	Interaction
Body weight (g)	202±3†,‡	370±6	351±7	365±12	383±9^{+}	n.s.	n.s.	0.54
Heart weight (HW, mg)	889±18†,‡	1596±32	1412±53**	1757±27^{++}	1599±29**$^{,+++}$	<0.001	<0.001	n.s.
HW/TL (mg/mm)	24.1±0.5†,‡	39.7±0.9	35.2±1.3**	42.3±0.7^{+}	38.1±0.6**$^{,+}$	0.004	<0.001	n.s.
Lung weight (mg)	1104±19†,‡	2146±91	1896±116*	1973±59	1781±71	n.s.	0.014	n.s.
Lung weight/TL (mg/mm)	29.9±0.6†,‡	53.3±2.3	47.3±3	47.5±1.5	42.4±1.7	0.018	0.014	n.s.
Kidney weight (mg)	1779±40†,‡	3626±142	3195±69*	4386±172^{+++}	3692±143***$^{,+}$	<0.001	<0.001	n.s.
Kidney weight/TL (mg/mm)	48.1±1†,‡	90.1±3.7	79.5±1.6*	105.6±4.3^{++}	87.9±3.4**	0.002	<0.001	n.s.
Liver weight (g)	8.27±0.36†,‡	13.85±0.32	12.61±0.74	15.89±0.82^{+}	14.11±0.45*	n.s.	0.021	n.s.
Liver weight/TL (mg/mm)	223.7±9.4†,‡	343.9±8.3	313.9±17.9	383.4±21.6	336.2±10.9	n.s.	0.021	n.s.
Spleen weight (mg)	632±14†,‡	1046±51	900±37	1354±98^{++}	1009±60***	0.004	0.001	n.s.
Spleen weight/TL (mg/mm)	17.1±0.4†,‡	26±1.3	22.4±0.9	32.6±2.4^{++}	24±1.4**	0.007	0.013	0.05

[§]p-values of two-way ANOVA including two factors: (i) age (14 *vs.* 19 weeks) and (ii) treatment (high-salt control *vs.* high-salt + spermidine).

***p<0.001, **p<0.01, *p<0.05 *vs.* age-matched control (simple main effects following significant two-way ANOVA)

$^{+++}$p<0.001, $^{++}$p<0.01, $^{+\#}$p<0.05 *vs.* 14-week-old treatment-matched group (simple main effect following significant two-way ANOVA)

†p<0.001 and ‡p<0.001 *vs.* 14-week-old and 19-week-old controls, respectively (one-way ANOVA comparing all controls with post-hoc Tukey or Welch's test with post-hoc Games-Howell according to equality of variances)

Supplementary Table 16: Left ventricular hemodynamic parameters of *Dahl* salt-sensitive rats.

Control and spermidine-treated *Dahl* salt-sensitive rats fed a high-salt (8% NaCl) diet starting from the age of 7 weeks (see Fig. 4a for the feeding scheme) were used at the indicated ages. Abbreviations: BSA, body surface area; CI, cardiac index; dP/dt_{max}, peak rate of pressure rise; dP/dt_{min}, peak rate of pressure decay; Ea_i, arterial elastance for indexed volumes, EF, ejection fraction; ESP, end-systolic pressure; EDP, end-diastolic pressure; ESV_i, indexed end-systolic volume; EDV_i, indexed end-diastolic volume; P_{max}, maximum ventricular pressure; SV_i, indexed stroke volume; VVC, ventricular-vascular coupling; τ, Left-ventricular pressure decay time constant (according to Weiss' method); EDPVR β_i, exponential end-diastolic pressure-volume relationship chamber stiffness constant for indexed volumes; ESPVR Ees_i, linear end-systolic pressure-volume relationship slope for indexed volumes. Data show means ± s.e.m. of indicated number of rats analyzed per group.

	7-week-old (no high-salt)	**14-week-old (7 weeks high-salt)**		**19-week-old (12 weeks high-salt)**		**Two-way ANOVA[§]**		
	Control (N=10)	Control (N=9)	Spermidine (N=9)	Control (N=10)	Spermidine (N=10)	Age	Treatment	Interaction
BSA (cm^2)	314±3$^{\dagger\dagger\dagger, \ddagger\ddagger\ddagger}$	469±5	453±6	464±11	480±7^{+}	n.s.	n.s.	0.052
HR (bpm)	429±8	419±12	421±11	410±8	403±10	n.s.	n.s.	n.s.
EF (%)	85±1$^{\dagger, \ddagger\ddagger\ddagger}$	81±1	80±2	70±1^{+++}	72±2^{++}	<0.001	n.s.	n.s.
CI ($\mu l/min.cm^2$)	298±16$^{\dagger\dagger\dagger, \ddagger\ddagger\ddagger}$	207±8	211±4	167±8^{+++}	178±7^{++}	<0.001	n.s.	n.s.
SV_i ($\mu l/cm^2$)	0.70±0.04$^{\dagger\dagger\dagger, \ddagger\ddagger\ddagger}$	0.49±0.02	0.5±0.01	0.41±0.02^{+++}	0.44±0.02^{+}	<0.001	n.s.	n.s.
ESV_i ($\mu l/cm^2$)	0.12±0.01‡‡	0.11±0.01	0.13±0.01	0.18±0.01^{++}	0.17±0.02^{+}	<0.001	n.s.	n.s.
EDV_i ($\mu l/cm^2$)	0.82±0.05$^{\dagger\dagger\dagger, \ddagger\ddagger\ddagger}$	0.61±0.03	0.63±0.02	0.59±0.03	0.62±0.02	n.s.	n.s.	n.s.
P_{max} (mmHg)	112±4$^{\dagger\dagger\dagger, \ddagger\ddagger\ddagger}$	136±4	123±4*	151±5^{++}	145±3^{+++}	<0.001	0.012	n.s.
ESP (mmHg)	99±5‡‡‡	116±5	106±4	132±6^{+}	130±3^{+++}	<0.001	n.s.	n.s.
EDP (mmHg)	7±0.7$^{\dagger, \ddagger\ddagger}$	10±0.4	8.7±0.3	10.6±1	7.8±0.5**	n.s.	0.005	n.s.
Ea_i ($mmHg*cm^2/\mu l$)	147±11$^{\dagger\dagger\dagger, \ddagger\ddagger\ddagger}$	236±9	212±8	331±21^{+++}	298±15^{+++}	<0.001	0.042	n.s.
dP/dt_{max} (mmHg/s)	6840±358	6711±282	6409±169	7475±234^{+}	7314±260^{+}	0.001	n.s.	n.s.
dP/dt_{min} (mmHg/s)	-6966±377†	-5960±393	-5560±319	-6948±306^{++}	-6703±208^{++}	<0.001	n.s.	n.s.
τ (ms)	7.7±0.2$^{\dagger\dagger, \ddagger}$	9±0.3	8.7±0.3	8.7±0.3	8.3±0.3	n.s.	n.s.	n.s.
VVC	1.15±0.18	1.07±0.08	1.28±0.14	0.99±0.15	1.35±0.14	n.s.	0.043	n.s.
ESPVR Ees_i ($mmHg*cm^2/\mu l$)	162±22$^{\dagger\dagger, \ddagger\ddagger}$	254±24	269±31	317±48	393±33^{+}	0.016	n.s.	n.s.
EDPVR β_i ($\mu l/cm^2$)	1.31±0.16$^{\dagger\dagger\dagger, \ddagger\ddagger\ddagger}$	1.83±0.24	1.45±0.14*	2.85±0.42	1.93±0.26***	n.s.	<0.001	n.s.

[§]p-values of two-way ANOVA including two factors: (i) age (14 *vs.* 19 weeks) and (ii) treatment (high-salt *vs.* high-salt + spermidine).

***p<0.001, **p<0.01, *p<0.05 *vs.* age-matched control (simple main effects following significant two-way ANOVA)

$^{+++}$p<0.001, $^{++}$p<0.01, $^{+}$p<0.05 *vs.* 14-week-old treatment-matched group (simple main effect following significant two-way ANOVA)

†††p<0.001, ††p<0.01, †p<0.05 *vs.* 14-week-old control and ‡‡‡p<0.001, ‡‡p<0.01, ‡p<0.05 *vs.* 19-week-old control (one-way ANOVA comparing all controls with post-hoc Tukey or Welch's test with post-hoc Games-Howell according to equality of variances)

Note: for ESPVR Ees_i and EDPVR β_i, other parameters in the fitting equation (V_0 and α, respectively) were included as covariates using ANCOVA.

Supplementary Notes

Information on human data analysis

Study subjects. The Bruneck Study is a prospective, population-based survey on the epidemiology and pathogenesis of atherosclerosis and cardiovascular disease[47,91–93]. At baseline in 1990 the study population comprised an age- and sex-stratified random sample of all inhabitants of Bruneck (125 men and 125 women from each of the fifth through eighth decades of age, all of Western European descent; 93.4% participated). In 1995, 826 subjects participated in the first quinquennial re-examination. During follow-up from 1995 to 2010, detailed information on fatal heart failure was carefully collected for all of these 826 subjects (follow-up rate, 100%). Population mobility in Bruneck is very low (<1% per year) and virtually all inhabitants are referred to one local hospital that closely works together with the general practitioners, which allows retrieval of full medical information. In 2010, 484 subjects were still alive and participated in the 4th re-evaluation. The study protocol was approved by the ethics committees of Bolzano and Verona and conforms to the Declaration of Helsinki. All study subjects provided written informed consent. Risk factors were assessed by means of validated standard procedures as described previously[47,91–93].

Quantification of nutritional intakes. Long-term average dietary intakes were ascertained in 1995, 2000, and 2005 by a dietitian-administered 118-item food frequency questionnaire (FFQ). This questionnaire was based on the gold standard FFQ by Willett and Stampfer[53] and modified to better fit the dietary peculiarities in the survey area. For each item in the FFQ a common unit or portion size was specified and participants declared their average intake by choosing one of nine response categories ranging from 'never' to 'six or more times a day'. Dietitians made use of illustrative photos of food items when exploring aphasic patients and of information provided by spouses, care-givers and nursing homes when dealing with demented and institutionalized subjects. An open-ended section inquired about foods not listed in the FFQ that were consumed at least once a week. Complex foods were dissected into component foods according to common recipes. Intakes of nutrients were calculated as weighted sums of food intakes using the United States Department of Agriculture nutrient database, release 23 (*U.S. Department of Agriculture, Agricultural Research Service. 2010. USDA National Nutrient Database for Standard Reference, Release 23. Nutrient Data Laboratory Home Page, http://www.ars.usda.gov/ba/bhnrc/ndl*). Special nutrient data were compiled for various supplements and for polyamines (see Nutrient Database Table below), also integrating a published database[94]. The FFQ was validated using full diet records over 7 to 9 days in 124 representative unselected subjects. Validity was high and similar to that previously reported for the same FFQ in other populations[83]. As expected and shown previously, dietary patterns were highly stable over time, corroborating that surveyed intakes are representative of average long-term intakes. This also applied to polyamine intakes with average correlation coefficients between successive assessments of spermidine, spermine, and putrescine of 0.54, 0.43, and 0.44, respectively. Overall, 2540 diet records were collected from 829 individuals who participated in at least one of the dietary assessments in 1995, 2000, 2005 and 2010. Out of this, 815 complete diet records were assessed in 1995 and 484 in 2010.

Ascertainment of the clinical end points. Between baseline (1995) and 2010, we collected detailed information on the time, cause, and circumstances of death of all study subjects who died during the follow-up period. Utilizing death certificates, all medical records ever compiled on study subjects, and autopsy reports in the rare event of unexpected death allowed complete ascertainment of deaths and reliable categorization of their causes. Death due to heart failure was defined according to ICD-10 diagnosis codes I50.x, I13.0, I13.2, I11.00, I11.01, and I97.1 (heart failure following cardiac surgery or due to presence of cardiac prosthesis). Clinically overt heart failure was defined according to gold standard Framingham criteria (presence of at least 2 major criteria or 1 major criterion in conjunction with 2 minor criteria)[84] and ascertained as part of the 2010 re-examination of the Bruneck Cohort. Causes of death as well as clinically overt heart failure were categorized by a senior researcher who was unaware of the dietary data.

Statistical analysis. Dietary intakes were cumulatively averaged over follow-ups to capture long-term dietary behavior and to reduce within-subject variability: For each follow-up and each subject, intakes assessed at that and all preceding follow-ups were averaged. Polyamine intakes were log-transformed and adjusted for total caloric intake by using the residual method[86] in a log-log simple linear model. They were then scaled to unit variance such that effects were estimated for one-standard deviation increases in intakes. Cumulatively averaged polyamine intake was used for the analyses targeting (a) the plasma proteome (2000) (b) overt heart failure (2010), and (c) blood pressures levels. Outcome analyses on cardiovascular disease used standard Cox models while outcome analysis on death due to heart failure employed the Fine and Gray proportional sub-distribution hazards model[95], accounting for the competing risk of death due to causes other than heart failure. Both time to event analyses (i.e. incident CVD and death due to heart failure) focused on the 15-year follow-up between 1995 and 2010 and used baseline (1995) polyamine intake as the exposure. Cross-sectional (2010) analysis on clinically overt heart failure employed unstratified logistic regression. Results on heart failure are presented without adjustment and with adjustment for age, sex, total caloric intake, current smoking, diabetes, alcohol consumption, and diastolic blood pressure (multivariable model). Analyses on blood pressure employed cumulatively averaged polyamine intakes from all four follow-ups in linear mixed models adjusting for age, age squared, sex, and total caloric intake. Multivariable adjustment (see above) resulted in very similar results (data not shown). Normality of residuals was investigated using normal quantile-quantile plots and deemed appropriate. The numbers of unique subjects and of diet records used for this analysis were 829 and 2540. All P values are two-sided and an alpha level of 0.05 is used throughout. Analyses were conducted with R 3.1.1.

Study characteristics: Participants were evaluated regarding their medical history, life-style behaviors, and vascular risk factors using standardized questionnaires and interviews. Individuals were coded as current smokers or non-smokers (including former smokers). Alcohol intake was quantified in grams per day. Systolic and diastolic blood pressures were taken after the participant had been sitting for at least 10 minutes and the mean of three independent measurements was calculated. Hypertension was defined as the presence of a systolic blood pressure ≥140 mmHg or a diastolic blood pressure ≥90 mmHg, or the use of antihypertensive drugs. Blood samples were taken in the morning hours after an overnight fast and 12 hours of abstinence from smoking and immediately processed or stored at -70 °C. *Diabetes mellitus* was diagnosed when fasting plasma glucose exceeded 126 mg/dl or when participants were under anti-diabetic medication.

Dietary Sources of Spermidine Intake in the Bruneck Cohort: Calculations are based on data obtained from 2540 food frequency questionnaires.

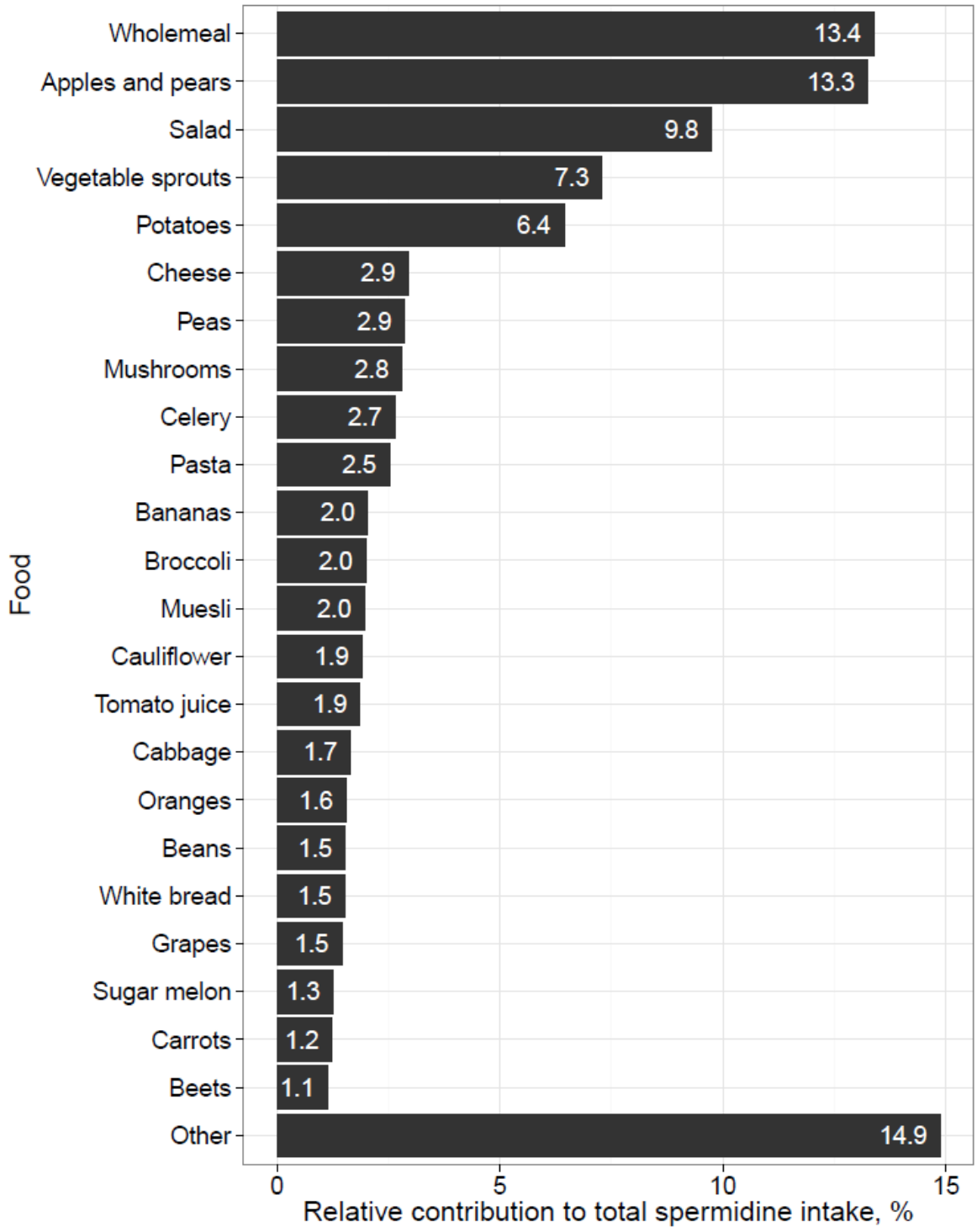

Nutrient Database for Polyamine Intake (in nmol/g).					
Food Category	**Spermidine**	**Spermine**	**Putrescine**	**Data points***	**Reference**
1. Milk and Dairy products					
Full cream milk	2	2	0	3	96
Skim milk	3	1	2	1	96
Yoghurt	2	1	1	3	97
Curd	0	0	0	1	97
Cheese†	113	23	876	19	96–98
2. Fruits					
Grapes	87	0	106	1	97
Apples	193	71	144	2	96
Peaches or apricots	42	25	4	1	97
Oranges	35	2	1302	4	98
Citrons	34	9	466	1	97
Water melon	8	0	0	1	97
Sugar melon	81	0	5	1	97
Strawberries	41	0	11	1	97
Blackberries	35	0	11	1	97
Prune (dried)	11	0	12	1	97
Pineapple	30	0	46	1	97
Mango	198	16	903	1	97
Cherry	19	0	53	1	97
Banana	60	0	323	1	97
3. Vegetables					
Tomato	20	1	347	4	98
Tomato sauce	58	0	294	1	96
Cucumber	44	3	75	3	98
Salad	150	23	85	9	97,98
Cabbage	82	8	86	1	96
Broccoli	309	46	113	3	96
Cauliflower	207	30	49	5	96
Carrots	46	2	56	7	99
Turnips	92	0	27	1	97
Peas	449	260	64	1	96
Kidney beans	134	120	4	1	96
Lentils	60	0	65	1	99
Spinach, uncooked	185	18	50	1	97
Spinach, cooked	50	11	146	1	96
Celeriac	184	n.d.	69	1	96
Garlic	181	20	21	2	97
Mushrooms	651	0	119	8	97
Wheat germs	2440	721	706	1	97
4. Protein					
Eggs	0	1	2	2	96
Poultry	37	314	12	4	96

Beef or veal	45	157	78	5	98
Pork	22	185	15	4	98
Game	106	287	251	3	96
Lamb, mutton and fawn-meat	34	233	11	1	97
Sausages (mortadella, wiener, chorizo)	28	106	585	4	96,98
Smoked ham	17	224	47	1	96
Innards (chicken, pork, beef)	240	606	96	9	97,99,100
Tuna	23	39	23	2	96
Freshwater fish	54	65	8	1	96
Saltwater fish	25	26	119	9	96-98
Soybean	854	192	332	4	96,97
Nuts	252	110	90	6	97
5. Sweets					
Chocolate	n.d.				
Confection of pastry	n.d.				
Ice	n.d.				
Goodies and candies	n.d.				
Honey	0	0	0	1	97
Cookies	n.d.				
6. Carbohydrate					
White bread	35	18	19	1	96
Whole-grain bread	129	36	24	2	98
Noodles	49	58	12	1	96
Dumplings	n.d.				
Cereals mixed	167	32	24	1	96
Potatoes	96	9	118	4	96
Rice	16	15	9	3	96,97
Polenta	297	6	520	1	97
Omelet	64	17	28	1	
Pizza dough‡	Similar to white bread data				
Chips	171	13	245	1	96
Potato chips	259	23	455	1	96
7. Butter, Oils and Cooking Fats					
Butter	n.d.				
Lard	n.d.				
Margarine	n.d.				
Olive oil	n.d.				
Seed oil	n.d.				
Mayonnaise	n.d.				
8. Drinks					
Cola	0	0	0	1	97
Lemonade	n.d.				
Apple juice	n.d.				
Lemon juice	n.d.				
Orange juice	13	0	621	1	98
Mineral water	0	0	0	1	

Red wine	2	0	83	4	98
White wine	0	0	44	2	97
Beer	3	0	189	3	97
Liquor, Schnapps	0	0	0	2	97
Coffee	0	0	1	1	96
Black tea	4	6	3	2	96
Green tea	23	19	18	1	97
Tea, general	1	0	0	1	96

*The table integrates published data from previous publications as indicated. Polyamine contents of similar types of food that matched the same FFQ food categories (manually curated) were grouped by using the mean or median of the group (the number of independent data points from matching food items is indicated). Zero values refer to polyamine contents below detection limit. Values are means except for mushrooms and nuts for which medians were used due to high variations within the available published data.

† 19 sorts of cheese excluding Cheddar.

‡ Replaced as indicated.

Supplementary References

89. *International Classification of Rodent Tumors. The Mouse*. (Mohr, Ulrich (Ed.), Springer Berlin Heidelberg, 2001).
90. Mi, H., Muruganujan, A. & Thomas, P. D. PANTHER in 2013: modeling the evolution of gene function, and other gene attributes, in the context of phylogenetic trees. *Nucleic Acids Res.* **41,** D377-386 (2013).
91. Kiechl, S. *et al.* Toll-like receptor 4 polymorphisms and atherogenesis. *N. Engl. J. Med.* **347,** 185–192 (2002).
92. Kiechl, S. *et al.* Blockade of receptor activator of nuclear factor-κB (RANKL) signaling improves hepatic insulin resistance and prevents development of diabetes mellitus. *Nat. Med.* **19,** 358–363 (2013).
93. Willeit, K. *et al.* Carotid atherosclerosis and incident atrial fibrillation. *Arterioscler. Thromb. Vasc. Biol.* **33,** 2660–2665 (2013).
94. Zoumas-Morse, C. *et al.* Development of a polyamine database for assessing dietary intake. *J. Am. Diet. Assoc.* **107,** 1024–1027 (2007).
95. Fine, J. P. & Gray, R. J. A Proportional Hazards Model for the Subdistribution of a Competing Risk. *J. Am. Stat. Assoc.* **94,** 496 (1999).
96. Kalač, P. & Krausová, P. A review of dietary polyamines: Formation, implications for growth and health and occurrence in foods. *Food Chem.* **90,** 219–230 (2005).
97. Nishimura, K., Shiina, R., Kashiwagi, K. & Igarashi, K. Decrease in Polyamines with Aging and Their Ingestion from Food and Drink. *J. Biochem. (Tokyo)* **139,** 81–90 (2006).
98. Eliassen, K. A., Reistad, R., Risøen, U. & Rønning, H. F. Dietary polyamines. *Food Chem.* **78,** 273–280 (2002).
99. Kala, P. Contents of polyamines in selected foods. *Food Chem.* **90,** 561–564 (2005).
100. Kalač, P. Recent advances in the research on biological roles of dietary polyamines in man. *J Appl Biomed* **7,** 65–74 (2009).